
Masters Theses

Student Theses and Dissertations

Summer 2020

Optical fiber based integrity test of civil engineering materials: Numerical analysis

Ruoyu Zhong

Follow this and additional works at: https://scholarsmine.mst.edu/masters_theses



Part of the [Civil Engineering Commons](#)

Department:

Recommended Citation

Zhong, Ruoyu, "Optical fiber based integrity test of civil engineering materials: Numerical analysis" (2020). *Masters Theses*. 8011.

https://scholarsmine.mst.edu/masters_theses/8011

This thesis is brought to you by Scholars' Mine, a service of the Missouri S&T Library and Learning Resources. This work is protected by U. S. Copyright Law. Unauthorized use including reproduction for redistribution requires the permission of the copyright holder. For more information, please contact scholarsmine@mst.edu.

OPTICAL FIBER BASED INTEGRITY TEST OF CIVIL ENGINEERING

MATERIALS: NUMERICAL ANALYSIS

by

RUOYU ZHONG

A THESIS

Presented to the Graduate Faculty of the

MISSOURI UNIVERSITY OF SCIENCE AND TECHNOLOGY

In Partial Fulfillment of the Requirements for the Degree

MASTER OF SCIENCE IN CIVIL ENGINEERING

2020

Approved by:

Wen Deng, Advisor

Hongyan Ma

Xiong Zhang

© 2020

Ruoyu Zhong

All Rights Reserved

PUBLICATION THESIS OPTION

This thesis consists of the following two articles, formatted in the style used by the Missouri University of Science and Technology:

Paper I: Pages 4-25 have been submitted to *Advances in Materials Sciences and Engineering Journal*.

Paper II: Pages 26-45 are intended for submission to *Frontiers Journal*.

Paper III: Pages 46-68 are intended for submission to *Sensors Journal*.

ABSTRACT

Major advancement in Civil Engineering cannot be accomplished without the help of sensors. Among different types of sensors, fiber-optic sensor is known for its light weight, high accuracy, resolution, immunity to electromagnetic interference, and resistance to harsh environment. This research mainly focuses on fiber-optic sensor application on concrete structures as temperature sensor. Thermal Integrity Profiling (TIP) is a non-destructive integrity testing method which makes use of the hydration heat from the concrete curing process to detect defects within a drilled shaft. Any defect of concrete could result in a temperature anomaly in a drilled shaft. The accuracy of the current method to measure temperature distribution within the concrete shaft is limited by the interval between sensors. To improve it, we implement fiber-optic sensor with high spatial resolution as thermal sensor. The flexibility of fiber-optic sensor allows it to be wrapped spirally around the reinforcement cage. Both changes to the method provide a more comprehensive temperature distribution data. Current method to interpret the data is so-called effective radius method. This method could underestimate the size of defect, especially an inclusion defect. We propose a new method to estimate the location and size of defect based on the high-resolution temperature distribution data measured by fiber-optic sensor. Moreover, we also take into account of the effect of aggregate in this study. Concrete is not a homogeneous material by containing aggregates with different size, shape and distribution. In this study, we investigate how the existence of coarse aggregate may affect the result. Countermeasure to minimize the effect of aggregate on thermal data interpretation is also proposed in this research.

ACKNOWLEDGMENTS

This thesis and related research are the result of work that has resulted in improving the fiber-optic sensor application on concrete structure that not only improves the test data quality but also the way of interpretation. The culmination of this work would not have been possible without contributions from the following:

Department of Civil, Architectural and Environmental Engineering, Missouri University of Science and Technology.

Wen Deng, Ph.D. – advisor

Xiong Zhang, Ph.D., P.E. – committee member

Hongyan Ma, Ph.D. – committee member

Ruichang Guo, Ph.D. – research associate

Chao Zeng, Ph.D.- research associate

Huanhuan Xia – research associate

Xiaobin Zhong – my father

Yuxia Zhong – my mother

TABLE OF CONTENTS

	Page
PUBLICATION DISSERTATION OPTION.....	iii
ABSTRACT.....	iv
ACKNOWLEDGMENTS	v
LIST OF ILLUSTRATIONS	ix
LIST OF TABLES	xi
NOMENCLATURE	xii
 SECTION	
1. INTRODUCTION.....	1
 PAPER	
I. OPTICAL FIBER BASED SMART CONCRETE THERMAL INTEGRITY PROFILING: AN EXAMPLE OF CONCRETE SHAFT.....	4
ABSTRACT	4
1. INTRODUCTION.....	5
2. METHODOLOGY.....	9
2.1. GOVERNING EQUATION.....	9
2.2. HEAT GENERATION	9
2.3. HEAT TRANSFER.....	10
2.4. HEAT CAPACITY	11
2.5. SIMULATION PARAMETERS.....	12
3. RESULT AND DISCUSSION	14

3.1. LOCATION PREDICTION	15
3.2. SIZE SENSITIVITY	18
4. CONCLUSIONS	22
REFERENCES	23
II. INVERSE MODELING OF FIBER-OPTIC BASED THERMAL INTEGRITY PROFILING.....	26
ABSTRACT	26
1. INTRODUCTION.....	27
2. METHODOLOGY.....	29
2.1. GOVERNING EQUATION.....	29
2.2. HEAT PRODUCTION	30
2.3. HEAT TRANSPORT.....	31
2.4. HEAT CAPACITY	32
2.5. SIMULATION PARAMETERS	32
3. RESULT AND DISCUSSION	34
3.1. NECKING	35
3.2. INCLUSION.....	38
4. CONCLUSIONS.....	44
REFERENCES	45
III. INFLUENCE OF AGGREGATES IN CONCRETE ON OPTICAL-FIBER BASED THERMAL INTEGRITY PROFILING ANALYSIS	46
ABSTRACT	46
1. INTRODUCTION TO EFFECT OF AGGREGATES	47
2. METHODOLOGY.....	50

2.1. GOVERNING EQUATION.....	50
2.2. HEAT TRANSFER IN AIR.....	50
2.3. HEAT GENERATION.....	51
2.4. HEAT TRANSFER IN SOIL.....	52
2.5. AGGREGATE DISTRIBUTION.....	54
2.6. SIMULATION PARAMETERS AND MODEL FOR BEAM.....	55
2.7. SIMULATION PARAMETERS AND MODEL FOR SHAFT.....	56
3. RESULT AND DISCUSSION.....	59
3.1. RESULT OF SELF-CONSOLIDATING CONCRETE BEAM.....	59
3.2. RESULT OF CONVENTIONAL CONCRETE BEAM.....	61
3.3. SHAFT MODEL.....	64
4. CONCLUSIONS.....	65
REFERENCES.....	66
SECTION	
2. CONCLUSION.....	69
VITA.....	71

LIST OF ILLUSTRATIONS

PAPER I	Page
Figure 1. Different kinds of defect	6
Figure 2. Shaft-soil model 1.....	13
Figure 3. Flow chart 1.....	13
Figure 4. Schematic of defect location	15
Figure 5. Result of simulation with different location.....	17
Figure 6. Schematic of defect size.....	19
Figure 7. Result of simulation with different size.....	20
PAPER II	
Figure 1. Shaft-soil model 2.....	33
Figure 2. Flow chart 2.....	35
Figure 3. Temperature distribution of shaft with necking defect.....	36
Figure 4. Sketch of necking defect	37
Figure 5. Temperature change rate along the optical fiber	39
Figure 6. Comparison of measured temperature and inversed modeling	39
Figure 7. Temperature distribution of inclusion.....	40
Figure 8. Trend line connecting each bottom point.....	41
Figure 9. Sketch of inclusion	42
Figure 10. Comparison of measured temperature and inversed model of inclusion.....	43
Figure 11. Comparison of two different cross-section shape but similar area.....	43

PAPER III

Figure 1. Flow chart of aggregate placement.....54

Figure 2. Geometry of beam model.....56

Figure 3. Shaft-soil model 3.....57

Figure 4. Simulation flow chart.....59

Figure 5. Temperature distribution of beam model 161

Figure 6. Temperature distribution.....63

Figure 7. Temperature data of shaft model.....65

LIST OF TABLES

	Page
PAPER I	
Table 1. Soil properties 1	14
Table 2. Location determination by different method	18
Table 3. Size determination	21
PAPER II	
Table 1. Soil properties 2	34
PAPER III	
Table 1. Properties of each component in beam model	57
Table 2. Heat rate and duration	58
Table 3. Soil properties 3	58

NOMENCLATURE

Symbol	Description
k	Thermal conductivity ($W/(m \times K)$)
C_p	Heat capacity(kJ)/(kg \times K)
ρ	Density (kg/m ³)
Q	Heat (J)
α	Degree of hydration (%)
w/cm	Water to cement ratio (1)
S_w	Saturation degree (%)
w	Water content (%)

1. INTRODUCTION

Sensing method has been widely applied in many aspects of Civil Engineering. From site exploration to construction process, to structural health monitoring, sensing method makes countless process more effortless and cost effective. For site exploration, Cone Penetration Test (CPT) is a method that a cone assorted with multiple sensors penetrates the soil and measures soil properties like pore water pressure, resistance. The whole process is almost automatic. Engineers only needs to read and interpret data. For construction process, numerous non-destructive methods cannot be done without sensors. Cross-hole sonic logging (CSL), Impulse response, Gamma-gamma logging, these methods utilize sensor as a mean to generate signal and read signal in order to test the integrity of a concrete shaft, where visual inspection is not available. Structural Health Monitoring (SHM) is proposed to set up an automatic monitoring system with minimum labour which is able to continuously monitor the structural health and detect any displacement and damage that happens to the structural. Many advancements cannot be accomplished without the help of sensors.

Among different kinds of sensors, fiber-optic sensor is known for its high accuracy, resolution, immunity to electromagnetic interference and resistance to harsh environment. Fiber-optic has application in stress measuring, strain measuring. Proposals of using fiber-optic sensor in Structural Health Monitoring to monitor strain and displacement have been made in many papers. Another application of fiber-optic sensor is in temperature measuring. Since fiber-optic sensor is immune to electromagnetic interference, it is one of the preferred sensors in environment that involves inflammable material. The working principle of fiber-

optic sensors is that light is transmitted through optical fiber and affected by the change in the optical fiber or grating due to environment change. These changes will be detected by the receiver and quantitatively interpreted into desired data. Advances in fiber optic sensor makes it more tolerable to extremely high temperature, more accurate and have higher spatial resolution. Rayleigh scattering fiber-optic sensor has the accuracy of 0.1°C and the spatial resolution smaller than 1 cm. Pulse pre-pump Brillouin optical time domain analysis (PPP-BOTDA) can survive 1000°C and has the spatial resolution of 2cm over a measurement distance of 0.5 km. These advancements bring more opportunity for the further development of Civil Engineering.

This thesis mainly focuses on fiber-optic sensor application on concrete structure, especially concrete shaft, as temperature sensor. Thermal Integrity Profiling (TIP) is a non-destructive integrity testing method which proposed by Mullins of University of South Florida. It makes use of the hydration heat from the concrete curing process to detect defects within a drilled shaft. Any shortage of concrete results in lower temperature compared to intact region in a drilled shaft. Current state of practice uses thermal-couples or infrared thermometers as mean to measure temperature distribution. While this method is considered as an improvement since it can detect defect in concrete cover outside of reinforcement cage, the cost of the method and the large interval between the sensors limits its development. Therefore, we propose using fiber-optic thermal sensor to replace the conventional sensor. The advantages of this change are lower cost, higher accuracy and spatial resolution. Not only the sensor itself improves the method, but also the way we can deploy the sensor. The flexibility of fiber-optic sensor allows us to wrap the sensor around the reinforcement cage spirally, which further improve the spatial resolution. In Paper I,

we make a proposal changing the conventional sensor to fiber-optic sensor. Comparison of result from both fiber-optic sensor and conventional method is provided.

Currently, the way to interpret TIP temperature distribution data is effective radius method. This method relies on the concrete pouring log and measured average data to conduct a temperature-radius relationship. Then based on the relationship and the temperature distribution data, one can calculate the effective radius at each location and build an inverse shaft model. However, this method may underestimate the size of defect, especially the size of inclusion. Therefore, we propose a new method to estimate the size of defect based on the more comprehensive data acquired from fiber-optic sensor in Paper II. Models are built with different types of defect and simulated. Data is interpreted in the proposed method and used to build inversed models. Comparisons of the temperature between original model and inversed model is shown in Result and Discussion section. The estimation made by inverse modeling shows good agreement with the original model.

In Paper III, we give a length of discussion about the effect caused by aggregates. Concrete is not homogeneous material due to the size, shape and distribution of aggregates as well as the properties difference between cement and aggregates. However, current studies do not give enough attention to the effect of aggregates when they test the feasibility to apply fiber-optic sensor in concrete. The inhomogeneity of concrete may make it harder to detect damage that happens to concrete since the inhomogeneity can cause temperature variation just like defect can. Concrete structures with different size of aggregate are simulated using FEM method. The result is presented and method to minimize this effect is discussed as well.

PAPER

I. OPTICAL FIBER BASED SMART CONCRETE THERMAL INTEGRITY PROFILING: AN EXAMPLE OF CONCRETE SHAFT

ABSTRACT

Concrete is currently most widely used construction material in the world. The integrity of concrete during pouring process could greatly affect its engineering performance. Taking advantage of heat production during concrete curing process, we propose an optical-fiber based thermal integrity profiling (TIP) method which can provide a comprehensive and accurate evaluation of the integrity of concrete immediately after its pouring. In this paper, we use concrete shaft as an example to conduct TIP by using the optical fiber as temperature sensor which can obtain high-spatial-resolution temperature data. Our method is compared to current thermal infrared probe or embedded thermal sensor based TIP for concrete shaft. This innovation makes it possible to detect defects inside of concrete shaft with thorough details, including size and location. Firstly, we establish a 3D shaft model to simulate temperature distribution of concrete shaft. Then, we extract temperature distribution data at the location where optical fiber would be installed. Based on the temperature distribution data, we reconstruct a 3D model of concrete shaft. Evaluation of the concrete integrity and the existence of the potential defect are shown in the paper. Overall, optical-fiber based TIP method shows a better determination of defect location and size.

1. INTRODUCTION

Concrete is currently most widely used construction material all over the world. Concrete consists of both fine and coarse aggregates that are bonded by cement paste. Hydration reaction occurs when cement is blended with water. This hydration is an exothermal reaction, which means it generate heat and results in temperature rise with concrete curing. At the beginning, tricalcium aluminate (C3A) reacts with water and generates a large amount of heat, but the reaction would not last long. It is followed with a short period that release less heat called dormant phase. After a short period of dormancy, the alite and belite start to react and continuously generate heat. The maximum heat generation would last 10 to 20 hours after pouring. Since cementitious material can generate a large amount of heat, defects of concrete would lead to temperature divergence in the concrete structure. By taking advantage of such a feature of concrete, we propose an innovative method as optical-fiber based thermal integrity profiling (TIP) to inspect the concrete integrity and use the concrete shaft as an example to demonstrate the method.

Since concrete shaft serves as the deep foundation, quality of concrete shaft is critical for the safety of superstructures. Defects within concrete shaft would degrade the shaft performance (Figure 1). The existence of defects within concrete shaft is mainly due to some problems of construction and design deficiencies [1]. Among 5,000 to 10,000 shafts tested, 15% of shaft showed the deviation from ideal signal, 5% of tested shafts showed indisputable defect indication [2,3]. Since both excavation and concreting are blind processes when building drilled shafts, it is impossible to prevent defects from happening during construction completely. Determination of whether defects exist in concrete shaft

and how severe the defects are, are crucial to evaluate whether concrete shaft would satisfy its design purpose. Among the existing method, non-destructive testing is widely accepted method for shaft integrity test. Figure 1 shows different kinds of defect.



Figure 1. Different kinds of defect

Currently, major non-destructive testing methods include low strain integrity test and cross-hole sonic logging (CSL). Low strain integrity test, as known as sonic pulse echo method, use light hammer impacts and evaluate the collected force and velocity records to evaluate shaft integrity[4-6]. Low strain integrity test is cost-efficient and effective. However, this method has limitations including operator's familiarity and experience, and length/width ratio of concrete shaft. CSL is a widely used non-destructive integrity test method. For CSL, 3-8 access tubes must be installed within a shaft cross-section [7]. Then, a signal generator coupled with receiver is lowered, maintaining a consistent elevation, to test the integrity of concrete shaft. This method has higher accuracy but limited within the reinforcement cage. CSL method only tests the integrity of concrete shaft between the access tubes, while outside of that zone is left untested. However, the bending capacity of

concrete shaft is mainly depended on the outer part of concrete shaft. The core of concrete shaft has little contribution to bending capacity [8-9]. The integrity of outer part in concrete shaft should be evaluated as well.

TIP, which is a new non-destructive testing method, makes use of the hydration heat generated during concrete curing to determine whether defects exist and estimate their size and location according to the temperature distribution along the concrete shaft [10-12]. Temperature distribution is measured by lowering a thermal probe with infrared thermocouples into access tubes or by embedded thermal sensor during the curing process. Inverse modeling of temperature distribution would provide information whether the reinforcement cage has been misplaced, improper formation has happened. In addition, location and type of defect would be indicated from the data. A relative cool region indicates a shortage of concrete at that particular location whereas a relative warm region indicates extra concrete. Compare to previous methods, TIP covers a larger area and provides a more comprehensive result. However, due to the limited amount of access tube, temperature data for inverse modeling could be insufficient to accurately predict temperature distribution of the concrete shaft which could limit further development of this method [13,14].

Referring advancement in optical fiber studies, Rayleigh scattering caused by local refractive index fluctuations along the glass fiber can be used to measure strains and temperature. Every point on the optical fiber can send different Rayleigh scattering signal when subjected to temperature change, and therefore, every point along the fiber acts as a temperature sensor [15-19]. This feature of optical fiber makes it ideal temperature sensor to measure high spatial resolution temperature distribution. Currently, this technology has

been applied to measuring and recording temperature data, e.g., in car engines, microwave ovens or large furnaces for steel industry. Advances in the research on Rayleigh scattering based optical fiber make its application on TIP possible. By applying this optical fiber to TIP as temperature sensor, more comprehensive and consistent temperature data can be provided. The conventional method sets an access tube every 300mm diameter, and a measurement point within access tubes with vertical interval less than 500mm. In this optical-fiber based method, the optical fiber would be wrapped around reinforcement cage spirally and densely with negligible cost of fiber itself. Even if the vertical interval is the same as conventional method when wrapping the optical fiber, the horizontal interval would be still significantly smaller. Temperature data measured by optical-fiber based TIP would have high spatial resolution. Thus, the inverse modeling of temperature distribution can produce more reliable integrity report[20-22].

The objective of this paper is to address the advantages of our proposed optical-fiber based TIP method regarding its inverse modeling of temperature distribution of defected concrete shaft by having high resolution spatial temperature data. We used finite element method (FEM) to simulate temperature distribution of defected concrete shaft. Temperature data were extracted in two different ways based on the concepts of our new method and conventional infrared thermal probe method. Based on the temperature distribution data, we reconstructed the 3D geometry of concrete shaft based on two methods. The impact of size and location of defect on temperature distribution are discussed in this paper.

2. METHODOLOGY

In this section we will introduce the methodology for the simulation of shaft model.

2.1. GOVERNING EQUATION

The principle of TIP is to take advantage of correlation between the shape of concrete shaft and temperature distribution. Temperature distribution is simulated using FEM. The governing equation of temperature (T) distribution in concrete shaft is Equation (1)

$$\frac{\rho C_p \partial T}{\partial t} = \left[\frac{\partial}{\partial x} \left(k \frac{\partial T}{\partial x} \right) + \frac{\partial}{\partial y} \left(k \frac{\partial T}{\partial y} \right) + \frac{\partial}{\partial z} \left(k \frac{\partial T}{\partial z} \right) \right] + Q \quad (1)$$

where C_p represents the heat capacity of the material; k is the thermal conductivity of the material; Q is the heat source in the material.

2.2. HEAT GENERATION

The total amount of heat production and the rate of heat production are two important factors of temperature distribution. These two factors determine the temperature of the concrete shaft and the timing for TIP to be performed. The amount of heat and heat production rate are related to the ingredient of concrete. Concrete with different proportions would generate different amount of heat. To determine the total heat generation from concrete, one would need the composition of the concrete. Then based on the equation provided, the total heat production can be determined. The total heat production can be determined by Equations (2) to (3) [23]:

$$Q_0 = Q_{cem}p_{cem} + 461p_{slag} + Q_{FA}p_{FA} \quad (2)$$

$$Q_{cem} = 500p_{C_3S} + 260p_{C_2S} + 866P_{C_3A} + 420p_{C_4AF} + 624p_{SO_3} + 1186p_{FreeCaO} + 850p_{MgO} \quad (3)$$

The degree of hydration can be determined by the following equation (Schindler and Folliard, 2005; Mullins, 2010):

$$\alpha(t) = \alpha_u \exp\left(-\left[\frac{\tau}{t_e}\right]^\beta\right) \quad (4)$$

$$\alpha_u = \frac{(1.031w/cm)}{(0.194+w/cm)} + 0.5p_{FA} + 0.3p_{SLAG} \quad (5)$$

$$\beta = p_{C_3S}^{0.227} \cdot 181.4 \cdot p_{C_3A}^{0.146} \cdot Blaine^{-0.535} \cdot p_{SO_3}^{0.558} \cdot \exp(-0.647p_{SLAG}) \quad (6)$$

$$\tau = p_{C_3S}^{-0.401} \cdot 66.78 \cdot p_{C_3A}^{-0.154} \cdot Blaine^{-0.804} \cdot p_{SO_3}^{-0.758} \cdot \exp(2.187 \cdot p_{SLAG} + 9.5 \cdot p_{FA} \cdot p_{FACaO}) \quad (7)$$

where $\alpha(t)$ represents the degree of hydration of cement at time t . And w/cm is a water-cement ratio. β and τ are determined by the cementitious constituent fractions. According to ASTM D7949-14, the recommended timing to perform TIP would be 12 hours after concrete placement until the number of days equivalent to foundation diameter in meters divided by 0.3 m.

2.3. HEAT TRANSFER

Heat transport is another important factor for temperature evolution within concrete shaft. Heat is dissipated into surrounding soil after heat is generated due to hydration simultaneously. Heat transport includes three mechanisms: conduction, convection, and radiation. In this situation, heat conduction is predominant mechanism in heat transport. Heat conduction in the material is represented by thermal conductivity k .

Soil consists of solids, air, and water. The specific value of thermal conductivity of soil is determined by the constitution of soil and the thermal conductivity of each phase. The thermal conductivity can be determined by Equation (8) [24-26]

$$k_1 = k_s - n[k_s - S_w k_w - (1 - S_w)k_a] \quad (8)$$

where n denotes porosity, and S_w represents degree of saturation.

However, this model does not consider the effect caused by the shape of void inside of soil. Thus, they introduce a shape factor $\chi = \sqrt{S_w}$ into the equation to represent the effect caused by the shape of void. Then, the equation becomes:

$$k = \sqrt{S_w}\{k_s - n[k_s - S_w k_w - (1 - S_w)k_a]\} + (1 - \sqrt{S_w})k_a \quad (9)$$

2.4. HEAT CAPACITY

We assume the temperature of the soil is the same among three phases, and the heat capacity of the soil is also related to the three phases of soil. The heat required to raise the temperature of soil one degree can be calculated by $C_s m_s + C_w m_w + C_g m_g$. The total weight of the soil is $m_s + m_w + m_g$. The soil heat capacity can be determined as follow:

$$C_p = \frac{C_s m_s + C_w m_w + C_g m_g}{m_s + m_w + m_g} \quad (10)$$

Considering that the mass of air is negligible, the equation can be simplified as:

$$C_p = \frac{C_s + C_w w}{1 + w} \quad (11)$$

where w is water content.

2.5. SIMULATION PARAMETERS

A common concrete shaft consists of two parts: concrete and reinforcement cage. To get the data of temperature distribution, the sensor must be deployed inside of concrete shaft. As mentioned above, the optical fiber would be wrapped around reinforcement cage spirally so that temperature along the fiber would be obtained. When it comes to conventional TIP, temperature can only be measure through access tubes or at the points where embedded sensors are set.

In order to simulate the temperature evolution and distribution within the shaft, a 3D model is established as shown in Figure 2. The model consists of four parts: concrete inside reinforcement cage, concrete outside reinforcement cage, soil surrounding shaft, and soil below shaft. In this case, heat transfer into reinforcement cage has been neglected since reinforcement cage has low heat capacity, high thermal conductivity and relatively small volume.

However, simulation of reinforcement cage surface is still necessary, because reinforcement cage is where the optical sensor and access tubes are deployed. The location of reinforcement cage surface would be the interface between the core concrete cylinder and the concrete cover.

To get as much data as possible for high spatial resolution temperature distribution data, optical fiber is chosen to be deployed spirally. The pitch of optical fiber is 300 mm. To simulate access tubes in conventional TIP method, we use vertical lines to represent the access tubes. According to ASTM D7949-14, one access duct should be placed for every 300 mm in diameter. Therefore, there would 6 vertical lines on the reinforcement cage in our setting.

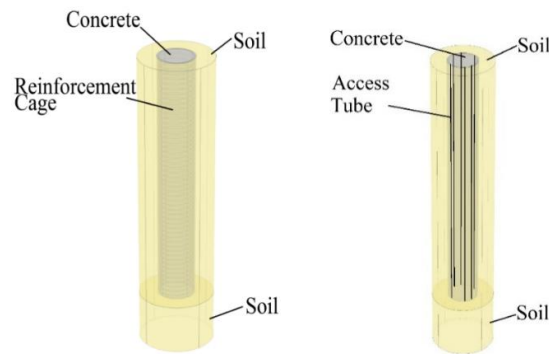


Figure 2. Shaft-soil model 1

The thickness of soil outside of concrete shaft is chosen based on the distance between two concrete shafts. In this case, the thickness is equal to the diameter of concrete shaft. The properties of soil are listed in the following Table 1. This simulation is conducted using FEM. The mesh type is free tetrahedral, with the minimum element size 0.21 m. Several defects would be set on the shaft. Size and location are important factors we will inspect when evaluating the quality of concrete shaft. In the simulation, the ability of the optical-fiber based TIP and the conventional TIP to detect defect size and location will be compared and discussed.

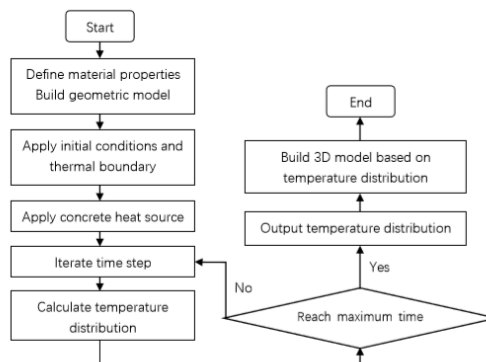


Figure 3. Flow chart 1

Table 1. Soil properties 1

Properties	Unit	Value
Density	kg/m^3	1800
Soil solid thermal conductivity	$W/m \cdot K$	5
Water thermal conductivity	$W/m \cdot K$	0.5
Air thermal conductivity	$W/m \cdot K$	0.05
Soil solid heat capacity	$J/(kg \cdot K)$	850
Water heat capacity	$J/(kg \cdot K)$	4190
Porosity	%	51.1
Water Content	%	39.8
Saturation	%	97

3. RESULT AND DISCUSSION

In this section, we discuss the result of simulations using two different ways to extract data based on the concept of different TIP methods. Location and size of the defects are considered. Firstly, we compare the results from two methods regarding how defect location will affect the result. Then, we investigate how defect size will affect the result. Figure 3 shows the steps of simulation.

3.1. LOCATION PREDICTION

When performing TIP method, we consider the location of the peak value as the location of the defect. To compare the accuracy of both methods, numerical simulation of a 6 feet diameter concrete shaft with 12 inches size cubic defect at selected locations is conducted. The location selected would be: defect is exactly at the measurement point of access tube method, defect is shifted from measurement point of access tube method, and defect is between measurement points of access tubes, separately (Figure 4). The result is shown in Figure 5, the concave region indicates the region that has negative value of temperature divergence. The region with dark blue color is the determination of defect by each method. The area of dark blue region indicates the size of defect, whereas the location of that region indicates the location of defect.

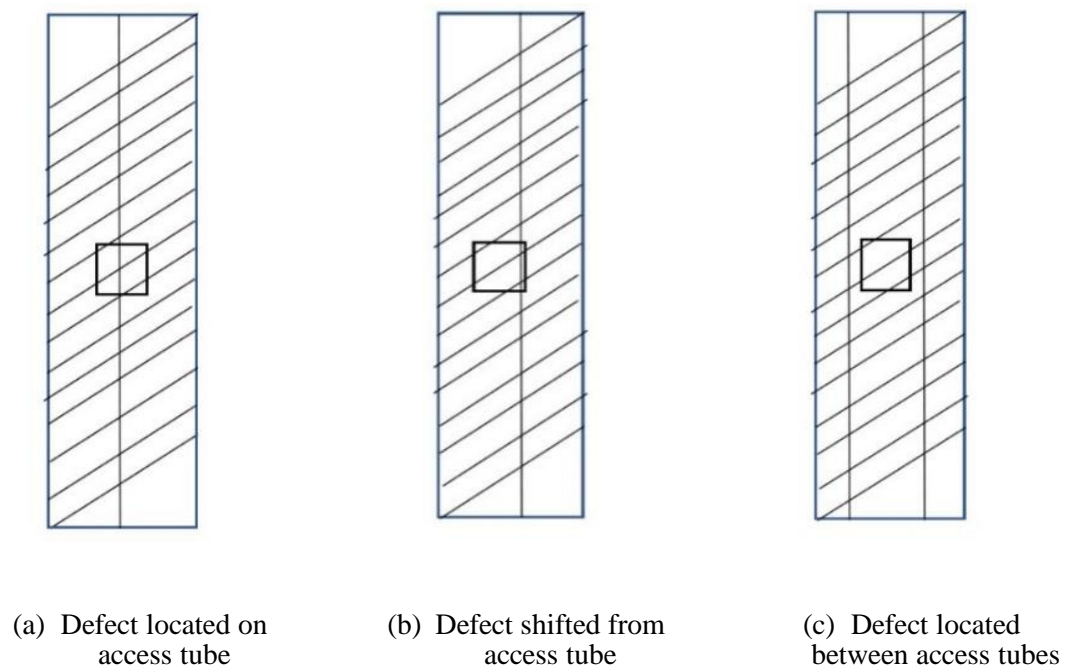


Figure 4. Schematic of defect location

When defect locates at the position where the infrared thermal probe measures temperature, both methods provide accurate determination of location. Furthermore, the temperature distribution can roughly indicate the shape of the defect. When defect is shifted from the position where the infrared thermal probe measures temperature, although both methods can detect the defect, the result from conventional TIP method deviates from the actual location of the defect.

At the same time, optical-fiber based TIP method can still have an accurate prediction of defect location. When defect happened to locate between two measurement points of conventional TIP method, although both methods can detect the defect, the result from conventional TIP method can hardly predict the location of defect. The temperature distribution between access tubes does not show significant peak value. The location of defect can be anywhere within the low temperature region. Optical-fiber sensor based TIP, on the other hand, can still have an accurate determination of defect.

According to the result presented in Table 2, in all three situations, optical-fiber based TIP method has great outcome despite the location of defect. The even distribution of measurement points and relative small interval not only increase the possibility of defect located at measurement but also diminish the effect when peak value doesn't locate at the measurement point, which contributes to more accurate reconstructed temperature distribution.

Considering that at most situation, defect doesn't locate exactly at the measurement method, we could draw a conclusion that optical-fiber based TIP method would always have same or better determination of defect location.

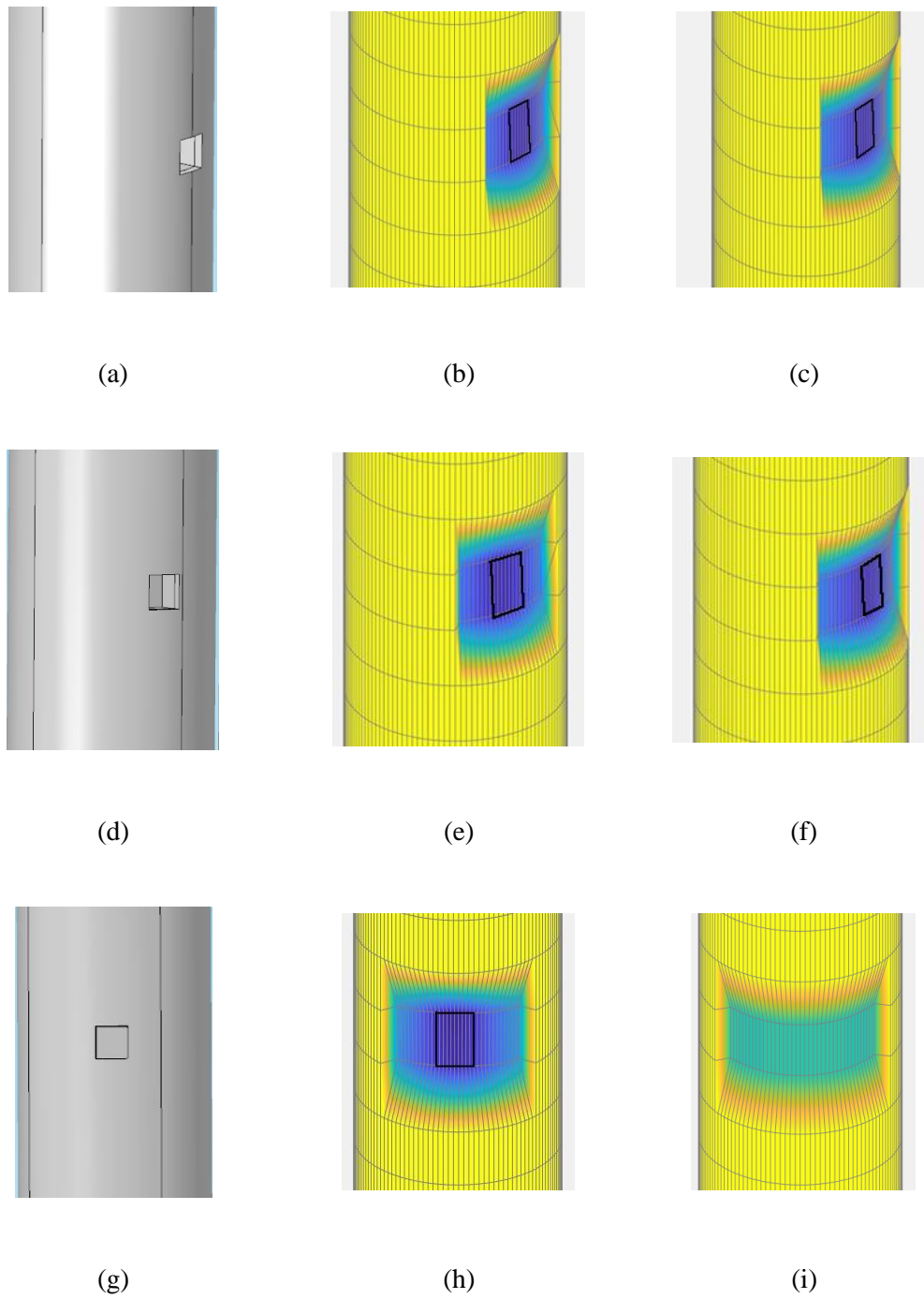


Figure 5. Result of simulation with different location.
 (a) (d) (g) actual location of defect, (b) (e) (h) location determination by optical-fiber method, (c)
 (f) (i) location determination by conventional method

Table 2. Location determination by different method

Situation	Actual location			Optical-fiber method			Conventional method		
	Depth	θ	r	Depth	θ	r	Depth	θ	r
On tube	7.5m	180	0.6096	7.58m	179.7	0.6148	7.58m	181	0.6148
Around tube	7.5m	171	0.6096	7.575m	169	0.6175	7.575m	179.7	0.619
Between tubes	7.5m	150	0.6096	7.576m	149.1	0.6096	N/A	N/A	0.774

3.2. SIZE SENSITIVITY

Size of the defect is also a significant factor needed to be considered for shaft integrity test. The size of defect is related to the magnitude of temperature divergence. The peak value of temperature distribution is crucial to determine the size of defect. To compare the accuracy of both methods, numerical simulation of a 6 feet concrete shaft is conducted with different defect of different size located between access tubes. The size of the defects are 18 inches, 15 inches and 10 inches, respectively (Figure 6). Anomaly that has 12% of area reduction is an anomaly needed for further evaluation. Both methods should have the ability to detect defect at this size.

The result is shown in Figure 7, the concave region indicates the region that has negative value of temperature divergence. The region with dark blue color is the determination of defect by each method. The area of dark blue region indicates the size of defect, whereas the location of that region indicates the location of defect.

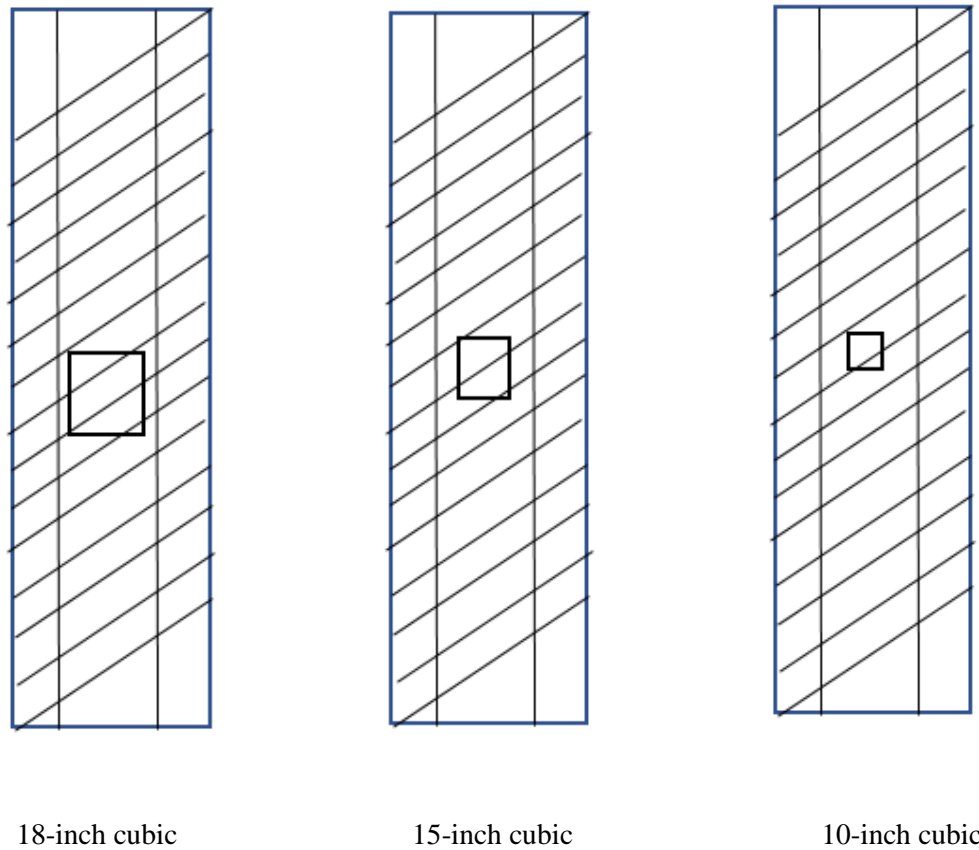


Figure 6. Schematic of defect size

When the defect is a 15-inch cubic at the lateral surface of concrete shaft, both methods can detect the existence of the defect. However, the optical-fiber method has a larger temperature divergence, closer to the actual temperature distribution in that region. When the defect is a 10-inch cubic at the lateral surface of concrete shaft, the infrared thermocouple probe or embedded sensor based TIP cannot detect defect between access tubes. The temperature divergence caused by defect would only maintain within a certain zone. Once the effect zone is located totally between access tubes, conventional TIP may miss the existing defect which may have negative effect on the performance of concrete shaft. The optical-fiber based TIP method still can detect defect.

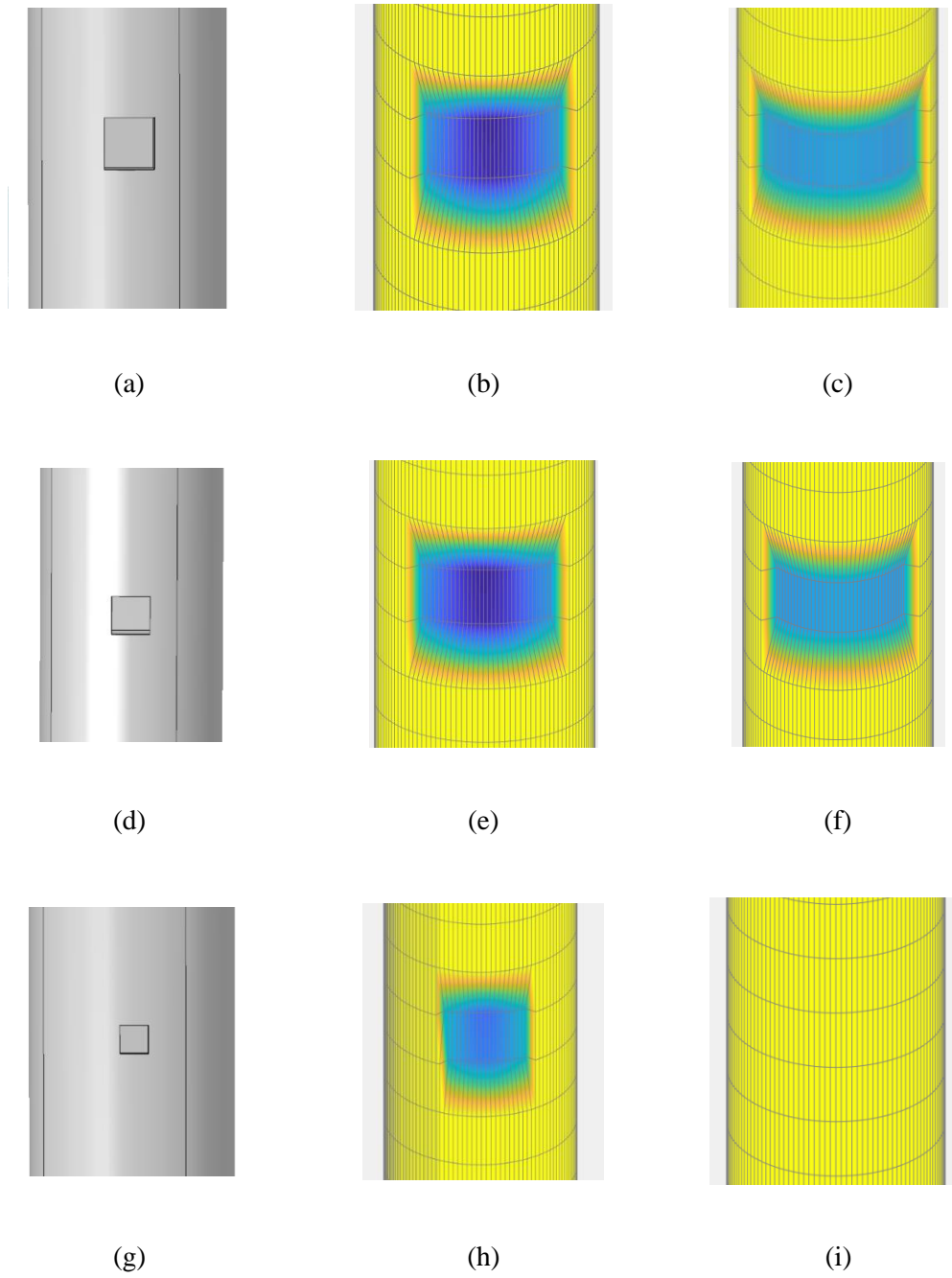


Figure 7. Result of simulation with different size.
 (a) (d) (g) actual size of defect, (b) (e) (h) size determination by optical-fiber method, (c) (f) (i) size determination by conventional method

The area of defect is smaller compared with the result shown in Figure 7, indicating that the size of the defect is smaller than the result shown in Figure 7. This demonstrates that TIP method has the ability to measure size based on the temperature distribution result. Table 3 shows the determination by both methods.

Table 3. Size determination

Actual Size	Optical-fiber method	Conventional method
18-inch cubic	17.60 inches	13.34 inches
15-inch cubic	14.68 inches	10.90 inches
10-inch cubic	9.84 inches	5.45 inches

Since size of defect is related to the magnitude of temperature divergence, accurate temperature distribution is crucial to the defect size evaluation. The value of peak temperature divergence decreases from the center of defect outward. As distance from center of defect increase, the temperature distribution would be closer to intact part. The closer the measurement point is to the center of defect, the higher accuracy of temperature distribution measurement would be. The conventional TIP has no measurement point between access tubes, which limits the minimum size of defect that can be detected. Optical-fiber based TIP, on the other hand, has the ability to detect smaller defect due to

high spatial resolution. However, if the size of defect is too small, even optical-fiber based TIP will not be able to detect.

4. CONCLUSIONS

In this section we proposed an optical-fiber based TIP method. This method can be an improvement of infrared thermocouple probes and embedded sensor which are applied to conventional TIP by having high spatial resolution temperature data. The method also changes the way to deploy sensor from separated vertically deployed to spirally deployed around reinforcement cage. These two changes enable TIP to measure a high resolution and consistent temperature distribution within concrete shaft, leading to more accurate determination of integrity of concrete shaft.

To verify the advantages of optical-fiber based TIP, we investigate two factors of defect: location and size. In the location section, we set three situations: defect on access tube, shift from access tube, between access tubes, respectively. When defect is located exactly on the access tube, both methods have an accurate determination of the location. However, when defect is located between access tube where conventional TIP doesn't have measure point, optical-fiber based TIP shows higher accuracy on location determination. We also simulate three situations with different size defects located between access tube. Since optical-fiber based TIP have measure point evenly distributed at the surface, the sensitivity of optical-fiber based TIP to the size of defect is significantly higher. In the simulation regarding the shape of defect, since measure point of optical-fiber based TIP distribute evenly within the defect, more precise outline of the defect is depicted by optical-

fiber based TIP. Overall, optical-fiber based TIP shows higher accuracy in prediction of shaft defects.

REFERENCES

- [1.]O'Neill M., "Integrity testing of foundations," *Washington, D.C.: Transportation Research Board*, pp. 6-13, 1991.
- [2.]Klingmuller O., and Kirsch, F., "Current practices and future trends in deep foundations," *Reston, VA: American Society of Civil Engineers*, pp. 205, 2004.
- [3.]Dan Brown, Anton Schindler, "High performance concrete and drilled shaft construction," *GSP 158 Contemporary Issues in Deep Foundations*, 2007.
- [4.]Massoudi, N., and Teffera, W. , "Non-destructive testing of piles using the low strain integrity method." *Proc. 5th Int. Conf. on Case Histories in Geotechnical Engineering*, Missouri Univ. of Science and Technology, Rolla, MO, 13–17,2004.
- [5.]Jeremy C. Ashlock, A.M. ASCE and Mohammad K. Fotouhi, "Thermal integrity profiling and crosshole sonic logging of drilled shafts with artificial defects," *Geo-Congress 2014 Technical Papers, GSP 234 © ASCE*, no. 1795, 2014.
- [6.]Sheng-Jen Hsieh, Robert Crane And Shamachary Sathish, "Understanding and predicting electronic vibration stress using ultrasound excitation, thermal profiling, and neural network modeling," *Nondestructive Testing and Evaluation*, vol. 20, no. 2, pp.89-102, 2005.
- [7.]D. Li, L. Zhang and W. Tang, "Closure to "reliability evaluation of cross-hole sonic logging for bored pile integrity," *Journal of Geotechnical and Geoenvironmental Engineering*, vol. 133, no. 3, pp. 343-344, 2007.
- [8.]Johnson, K. and Mullins, G., "Concrete temperature control via voiding drilled shafts," *Contemporary Issues in Deep Foundations, ASCE Geo Institute, GSP 158*, no. 1, pp. 1-12, 2007
- [9.]Kevin R. Johnson, MCE, E.I. "Temperature prediction modeling and thermal integrity profiling of drilled shafts," *Geo-Congress 2014 Technical Papers, GSP 234 © ASCE*, no.1781, 2014.
- [10.]G. Mullins, "Thermal Integrity Profiling of Drilled Shafts", *DFI Journal*, vol. 4, no. 2, pp. 54-64, 2010.

- [11.]Mullins, Gray . “Advancements in drilled shaft construction, design, and quality assurance: the value of research”. *Technical Paper. International Journal of Pavement Research and Technology*. vol. 6, no. 2, pp. 93-99, 2013.
- [12.]Johnson, Kevin R. “Analyzing thermal integrity profiling data for drilled shaft evaluation”. *DFI Journal – The Journal of the Deep Foundations Institute*. Vol. 10, no. 1, pp. 25-33,2016.
- [13.]Gray Mullins, “Advancements in drilled shaft construction, design, and quality assurance: the value of research,” *International Journal of Pavement Research and Technology*, vol. 6, no. 2, pp. 933-99, 2013
- [14.]Allen G. Davis, “Assessing reliability of drilled shaft integrity testing,” *Transportation Research Record 1633*, no. 98-0245.
- [15.]Dirk Samiec, “Distributed fiber optic temperature and strain measurement with extremely high spatial resolution,” *Polytech GmbH*, Waldbronn Germany, 2011.
- [16.]Wansheng Pei, Wenbing Yua, Shuangyang Li, etc. “A new method to model the thermal conductivity of soil–rock media in cold regions: An example from permafrost regions tunnel,” *Cold Regions Science and Technology*, no. 95, pp. 11-18, 2013.
- [17.]Travis J. Moore, MatthewR.Jones, DaleR.Tree, etc. “An inexpensive high-temperature optical fiber thermometer,” *Journal of Quantitative Spectroscopy & Radiative Transfer*, no.187, pp.358-363, 2017.
- [18.]Huaizhi Su, Jiang Hu, and Meng Yang, “Dam seepage monitoring based on distributed optical fiber temperature system,” *IEEE Sensors Journal*,Vol. 15, no. 1, pp. 9-13, 2015.
- [19.]Robert K. Palmer, Kelly M. McCary, and Thomas E. Blue , “An analytical model for the time constants of optical fiber temperature sensing,” *IEEE Sensors Journal*, Vol. 17, no. 17, pp.5492-5511, 2017.
- [20.]Arnaldo Leal-Junior, Anselmo Frizzera-Neto, Carlos Marques, “A polymer optical fiber temperature sensor based on material features,” *Sensors*, Vol. 2018, no. 301, pp. 1-10, 2018.
- [21.]Yi Rui, Cedric Kechavarzi, Frank O’Leary, “Integrity testing of pile cover using distributed fibre optic sensing,” *Sensors*, no.17, pp. 1-20, 2017.
- [22.]Yamile Cardona-Maya, Juan Fernando Botero-Cadavid. “Refractive index desensitized optical fiber temperature sensor,” *Revista Facultad de Ingeniería*, no. 85, pp. 86-90, 2017.
- [23.]Schindler and K. Folliard, "Heat of hydration models for cementitious materials", *ACI Materials Journal*, vol. 102, no. 1, pp 24-33, 2005.

- [24.]W. Liu, P. He and Z. Zhang, “A calculation method of thermal conductivity of soils,”*Journal of Glaciology and Geocryology*, vol. 24, no. 6, pp. 770-773, 2002.
- [25.]Cristina Sáez Blázquez, Arturo Farfán Martín, Ignacio Martín Nieto, etc. “Measuring of thermal conductivities of soils and rocks to be used in the calculation of a geothermal installation,” *Energies*, vol. 10, no. 795, pp. 1-19, 2017.
- [26.]D. Barry-Macaulay, A. Bouazza, R.M. Singh, “Thermal conductivity of soils and rocks from the Melbourne (Australia) region,” *Engineering Geology*, no.164, pp.131-138, 2013.

II. INVERSE MODELING OF FIBER-OPTIC BASED THERMAL INTEGRITY PROFILING

ABSTRACT

Current state of practice to interpret Thermal Integrity Profiling (also known as TIP) data is so-called effective radius method. It uses the concrete pouring log and average temperature to conduct relationship between temperature distribution and effective radius which can be used to reconstruct shaft model. While this method is computationally inexpensive and easy for use, it usually underestimates the size of inclusion. Changing the sensor used in conventional TIP to fiber-optic sensor provides more comprehensive temperature distribution data with higher accuracy and higher spatial resolution which makes it possible to further improve the interpretation method. In this study, we propose a back and forth modeling method. We reconstruction an intact shaft model and input defect. After simulation is done, we match the temperature distribution data with the original data and adjust the defect accordingly. Both necking and inclusion are simulated in this study to conduct new method of prediction of location and size of defect. The location of defect is represented by the spot that has lowest temperature measurement. The size of necking is described by two parameters on vertical direction and radial direction. The size of inclusion is described by an additional parameter at tangent direction. Result and comparison show that the predictions have good agreement with the original data.

1. INTRODUCTION

As mentioned in the previous section, concrete is one of the most widely used construction material in the world, from a basic house to high rise buildings. For the safe of the inhabitant inside, the inspection on concrete structure integrity is necessary. Within a concrete structure, concrete shaft bears the load from superstructures and transmits the load to the ground. However, studies show that such important structure has relative high rate of deficiency due to blind excavation and pouring process [2.3]. 15% of the concrete shafts among 5,000 to 10,000 tested showed signals of potential defects, 5% of the tested shaft had indisputable defect indication. Factors like slump, soft soil, inappropriate construction processes, cause the defect within a concrete shaft [1]. The lack of insurance for defect from happening makes the inspection afterward more significant for concrete shaft.

Among the inspection methods for concrete structure, non-destructive testing is the primary since it does not cause damage to the structure. Currently, major non-destructive testing methods include low strain integrity test and cross-hole sonic logging (CSL). Low strain integrity test, as known as sonic pulse echo method, use light hammer impacts and evaluate the collected force and velocity records to evaluate shaft integrity [4-5, 27]. Despite its merit in cost and time efficiency, low strain integrity test has limitations in the requirement for operators' experience and length/width ratio of concrete shaft. CSL uses acoustic energy to test whether there is any defect within the concrete shaft. The advantage of this method is high accuracy. Since the probe is lowered in the access tube preinstalled on the reinforcement cage, the tested area is limited between the access tube.

To have a more comprehensive method while keeping the merit of CSL, Thermal Integrity Profiling (TIP) is been proposed years ago as a new non-destructive testing method. TIP makes use of the hydration heat as a mean to test the structural integrity. Any defect would be shown as temperature anomaly in the data plot. This method enlarges the testing area from concrete within the reinforcement cage to concrete cover outside the cage.

TIP can also be a mean to estimate the size of defect size in concrete shaft. Current state of practice is to use concrete pouring log and average temperature measured to conduct a relation between average temperature and average radius. The temperature distribution plot along the radial direction at the cross-section is a bell shape plot. Temperature decrease as the measure point moves away from the center part. At the outer part of concrete shaft, the relationship between distance from center and temperature is almost linear. However, a line that fits the linear part of T-R curve with intercept the R-axial at a negative value. To simplify this method, a conservative fitting line is proposed by Johnson [8]. This line passes through the (T_{avg}, R_{avg}) and origin $(0,0)$ where R represents the distance from the center. This fitting line conducts a conservative prediction of defect compared to the conventional method and is easier to draw. Based on the effective radius calculated in this way, a 3-D geometry of concrete shaft can be established. While this method can roughly indicate the location and estimate the size of defect, the limited of convection TIP method may make the result less accurate, especially when the inclusion defect locates between the access tube.

The application of the fiber-optic temperature sensor on TIP can improve the data quality [28]. Fiber-optic sensor based TIP provides a more comprehensive data, with high accuracy and resolution. The small interval of the optical fiber and the way it is deployed

bring more accurate temperature data since it has higher chance to measure temperature distribution at the vicinity of defect. Based on this improvement, this study conducts a new method to estimate the location and size of the defect based on the temperature data. As discussed in the previous section, aggregates have negligible effect on the temperature distribution within the concrete shaft. Therefore, with the information such as cement composition, aggregate size and gradation, we can reconstruct a shaft model using FEM that has similar temperature distribution. Then, we extract information from the temperature data that is needed to reconstruct a similar defect. After simulating the reconstructed shaft model with defect, we compare the result and the measured temperature data. If the result shows a good agreement with the data, then the designed defect has the similar location and similar size as the defect in the actual shaft. This inverse modeling method can provide more information than the conventional effective radius method, especially for the inclusion case. In this study, simulation regarding the type of defect is established. Comparison of the result and the prediction based on the new method will be presented in the Result and Discussion section.

2. METHODOLOGY

In this section we will introduce the parameters and theories related to this research.

2.1. GOVERNING EQUATION

Since the Thermal Integrity Profiling relies on the heated by hydration in concrete and dissipated to the surrounding soil, the predominant physics involved is conduction

which is heat transfer way in solid. Thus, we use the heat transfer in solid module in Comsol to run the simulation to acquire temperature (T) distribution in concrete shaft. The governing equation of this module is Equation (1)

$$\frac{\rho C_p \partial T}{\partial t} = \left[\frac{\partial}{\partial x} \left(k \frac{\partial T}{\partial x} \right) + \frac{\partial}{\partial y} \left(k \frac{\partial T}{\partial y} \right) + \frac{\partial}{\partial z} \left(k \frac{\partial T}{\partial z} \right) \right] + Q \quad (1)$$

where C_p represents the heat capacity of the material; k is the thermal conductivity of the material; Q is the heat source in the material.

2.2. HEAT PRODUCTION

The heat production is significant to Thermal Integrity Profiling. The difference of heat production and dissipation combined results in temperature anomaly. Therefore, it is important to figure out the heat production before running simulation. The total amount of heat production and the rate of heat production together determine the temperature distribution of concrete shaft at a specific time. The amount of heat and heat production rate are related to the ingredient of concrete. The total heat production can be determined by Equations (2) to (4) [23]:

$$Q_0 = Q_{cem} p_{cem} + 461 p_{slag} + Q_{FA} p_{FA} \quad (2)$$

$$Q_{cem} = 500 p_{C_3S} + 260 p_{C_2S} + 866 P_{C_3A} + 420 p_{C_4AF} + 624 p_{SO_3} + 1186 p_{FreeCaO} + 850 p_{MgO} \quad (3)$$

$$Q_{FA} = 1800 p_{FACaO} \quad (4)$$

The degree of hydration can be determined by the following equation (Schindler and Folliard, 2005; Mullins, 2010):

$$\alpha(t) = \alpha_u \exp \left(- \left[\frac{\tau}{t_e} \right]^\beta \right) \quad (5)$$

$$\alpha_u = \frac{(1.031w/cm)}{(0.194+w/cm)} + 0.5p_{FA} + 0.3p_{SLAG} < 1 \quad (6)$$

$$\beta = p_{C_3S}^{0.227} \cdot 181.4 \cdot p_{C_3A}^{0.146} \cdot Blaine^{-0.535} \cdot p_{SO_3}^{0.558} \cdot \exp(-0.647p_{SLAG}) \quad (7)$$

$$\tau = p_{C_3S}^{-0.401} \cdot 66.78 \cdot p_{C_3A}^{-0.154} \cdot Blaine^{-0.804} \cdot p_{SO_3}^{-0.758} \cdot \exp(2.187 \cdot p_{SLAG} + 9.5 \cdot p_{FA} \cdot p_{FACaO}) \quad (8)$$

where $\alpha(t)$ represents the degree of hydration of cement at time t . And w/cm is a water-cement ratio. β and τ are determined by the cementitious constituent fractions.

2.3. HEAT TRANSPORT

On the top of the shaft model, heat dissipates into the air during the test. To take that into account, Heat flux boundary condition is defined at the top of the shaft. The heat flux boundary is assorted in Comsol. The only parameter needed is the temperature which is set to 23°C. In this situation, since no gas or liquid is involved in the model, heat conduction is main heat transport way in solid.

Soil is multi-phase material, consisting of solids, air, and water. The specific value of thermal conductivity k of soil is determined by the constitution of soil and the thermal conductivity of each phase. To simplify the model, we consider soil as one phase material and use effective thermal conductivity as its properties. The effective thermal conductivity can be determined by Equation (9) [23]

$$k_1 = k_s - n[k_s - S_w k_w - (1 - S_w)k_a] \quad (9)$$

where n denotes porosity, and S_w represents degree of saturation.

A shape factor $\chi = \sqrt{S_w}$ is introduced into the equation to represent the effect caused by the shape of void. Then, the equation becomes:

$$k = \sqrt{S_w}\{k_s - n[k_s - S_w k_w - (1 - S_w)k_a]\} + (1 - \sqrt{S_w})k_a \quad (10)$$

2.4. HEAT CAPACITY

We assume the temperature of the soil is the same among three phases, and the heat capacity of the soil is also related to the three phases of soil. The heat required to raise the temperature of soil one-degree can be calculated as the sum of the heat to raise one-degree of three phases separately, which in equation would be $C_s m_s + C_w m_w + C_g m_g$. The total weight of the soil is $m_s + m_w + m_g$. Therefore, the value of soil heat capacity can be determined as follow [24-26]:

$$C_p = \frac{C_s m_s + C_w m_w + C_g m_g}{m_s + m_w + m_g} \quad (11)$$

Considering that the mass of air is negligible, the equation can be simplified as:

$$C_p = \frac{C_s + C_w w}{1 + w} \quad (12)$$

where w is water content.

2.5. SIMULATION PARAMETERS

In order to simulate the temperature evolution and distribution within the shaft, a 3D model is established as shown in Figure 1. The model consists of three parts: concrete shaft, soil surrounding shaft, and soil below shaft. In this model, heat transfer into

reinforcement cage has been neglected since reinforcement cage has low heat capacity, high thermal conductivity and relatively small volume. Even though there is no actual reinforcement cage being input to the model, the location of reinforcement cage is still needed. To measure the temperature distribution within a concrete shaft, the sensor must be deployed inside of concrete shaft. To further improve the spatial resolution of TIP data, optical fiber is chosen to be deployed spirally around the reinforcement cage so that temperature along the fiber would be obtained. The vertical interval of optical fiber is 300 mm. For the similar reason as reinforcement cage, no actual fiber-optic sensor entity is input to the model. The thickness of soil outside of concrete shaft is as large as the diameter of concrete shaft. The properties of soil are listed in the Table 1.

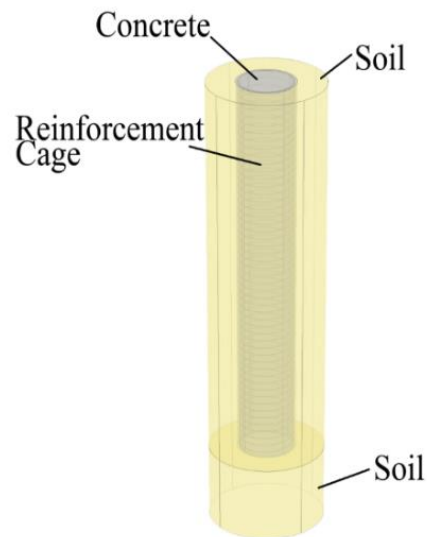


Figure 1. Shaft-soil model 2

This simulation is conducted using FEM. The mesh type is free tetrahedral, with the minimum element size 0.02 m. Several defects would be set on the shaft. Size and

location are important factors we will inspect when evaluating the quality of concrete shaft.

The simulation steps are shown in Figure 2.

Table 1. Soil properties 2

Properties	Unit	Value
Density	kg/m^3	1800
Soil solid thermal conductivity	$W/m \cdot K$	5
Water thermal conductivity	$W/m \cdot K$	0.5
Air thermal conductivity	$W/m \cdot K$	0.05
Soil solid heat capacity	$J/(kg \cdot K)$	850
Water heat capacity	$J/(kg \cdot K)$	4190
Porosity	%	51.1
Water Content	%	39.8
Saturation	%	97

3. RESULT AND DISCUSSION

In this section, results from simulations of different imperfect concrete shaft are presented. The defects include necking, inclusion. Following the proposed inverse

modeling method is an example of prediction using this method. Bulge is not discussed in this study since it is similar to the necking but only with opposite temperature anomaly. The method should work for the bulge case.

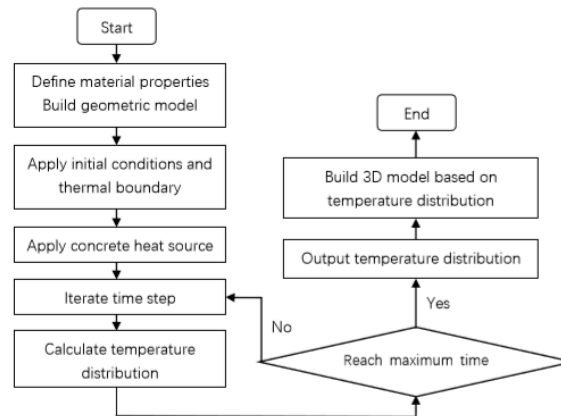


Figure 2. Flow chart 2

3.1. NECKING

Necking is defined as a rapid change of cross section. In the simulation, necking is presented as a cylinder with smaller radius connected with two cylinders with the designated radius of an intact shaft. A shortage of concrete means there would be less heat produced at that location. This results in a region where the temperature is lower than vicinity region. The result of the simulation is presented in Figure 3. As shown in the figure, temperature at the top and the bottom is smaller than the middle part. The reason is that heat can dissipate from top to the air and from bottom to the ground. The additional way to dissipate heat results in lower temperature even if the shaft is intact at that region. At the

middle of the figure, there is a region that shows lower temperature. That would be the location of necking in the simulated concrete shaft.

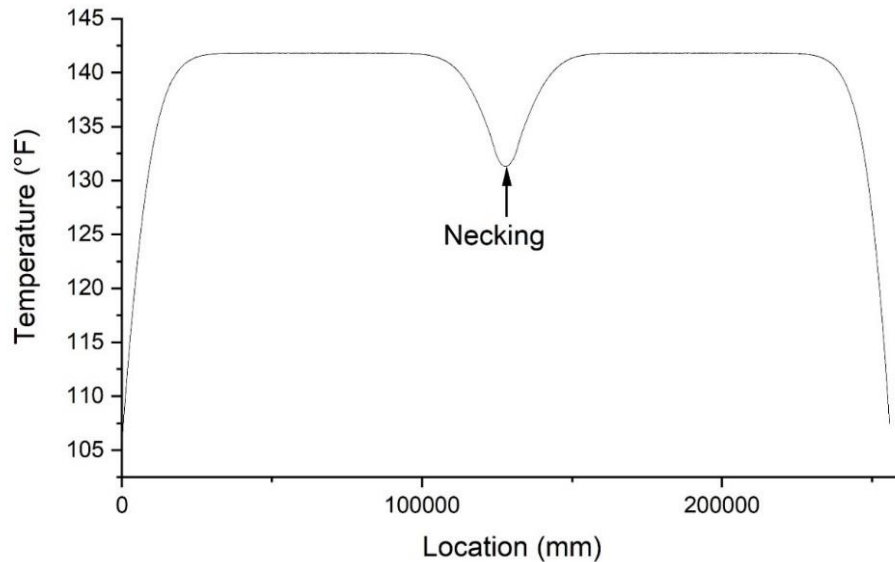


Figure 3. Temperature distribution of shaft with necking defect

From the figure, one can find that there is only one concave region which means there is only necking defect in the shaft. To separate necking from inclusion, one can calculate the length of the optical fiber that passes a single concave in the plot. If the length is larger than one or two perimeter of reinforcement cage with only one concave, the defect can be recognized as necking. If several concaves are presented continuously on the plot, one can recognize it as an inclusion defect.

To estimate the location of a necking, one can rely on the location that has the lowest temperature measurement shown in the plot. Optical fiber wrapped around the reinforcement cage passes through the effect region. As it passes around the vertical center

of the necking region, the temperature measurement reaches the bottom in the plot. The location can be calculated based on the x-axial on the plot. The x-axial represents the location on the optical fiber which can be converted to the location in the concrete shaft. The vertical location calculated from this method is the vertical center of the neck.

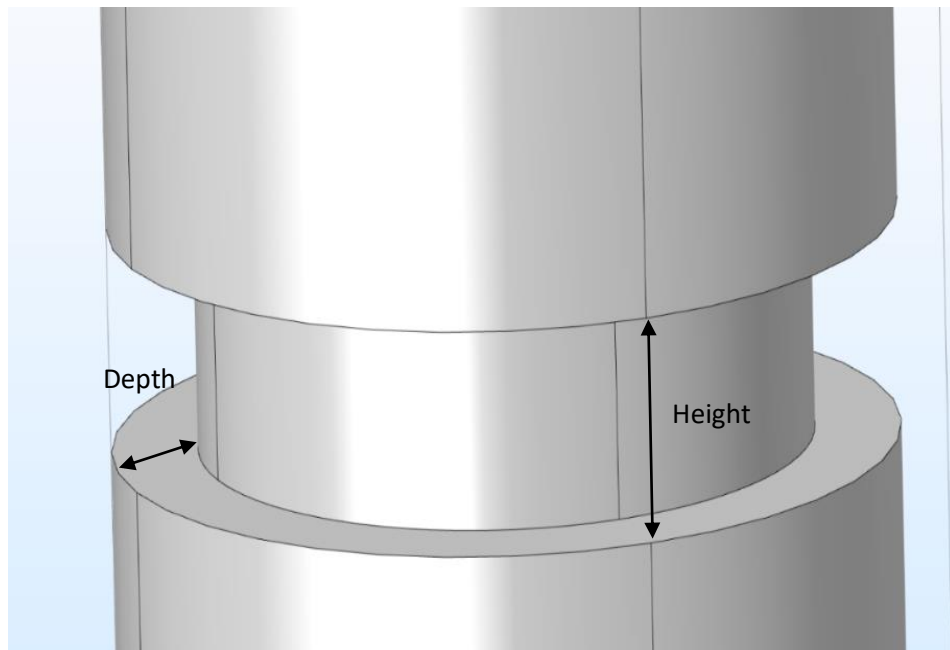


Figure 4. Sketch of necking defect

To reconstruct the defect, aside from the location, the size of the defect is also necessary. The size of a necking can be determined by two parameters, height at vertical direction and depth at radial direction, as shown in Figure 4. In the case of necking, effective radius calculated using the method proposed by Johnson [7] shows good agreement with the simulation. Thus, the depth can be determined by the effective radius. The height can be determined by the temperature data acquired by the optical fiber sensor.

Assuming that whenever the fiber-optic sensor passes the boundary of a defect, the slope of the temperature distribution plot will be the largest. After calculating the slope of the plot, at the region that has temperature anomaly caused by necking, there is a point intercepts with the x-axial which is the center of the temperature anomaly. As shown in Figure 5, these are two inflection points around the interception point with the lowest and the highest changing rate respectively. The locations of these two points determine the upper and lower boundary of the necking. The gap between the boundaries is the height of the necking. So far, we have the parameters needed to reconstruct the defect. The comparison between the temperature distribution of the reconstructed model and the original shaft model is presented in Figure 6.

3.2. INCLUSION

The temperature distribution of inclusion is shown in Figure 7. The temperature distribution plot of an inclusion defect consists of several concaves continuously. The inclusion only effects the temperature distribution of vicinity and the temperature distribution on the opposite side remains unchanged. Thus, the temperature distribution between concaves in Figure 7 is the same as the intact region. This can be the reference to separate a necking defect and an inclusion.

To determine the location of an inclusion, the method that applies for necking can also be used. Although the plot of temperature distribution of inclusion has more than one concave, the location of that has the lowest temperature measurement can still be an indication of the center of inclusion.

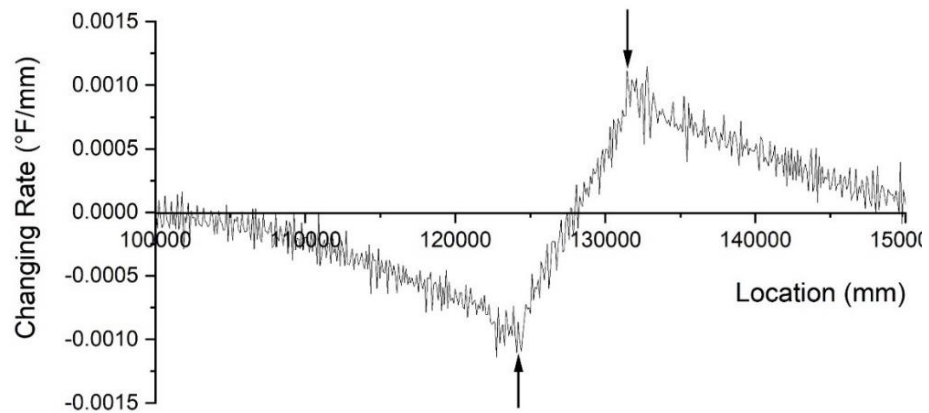


Figure 5. Temperature change rate along the optical fiber

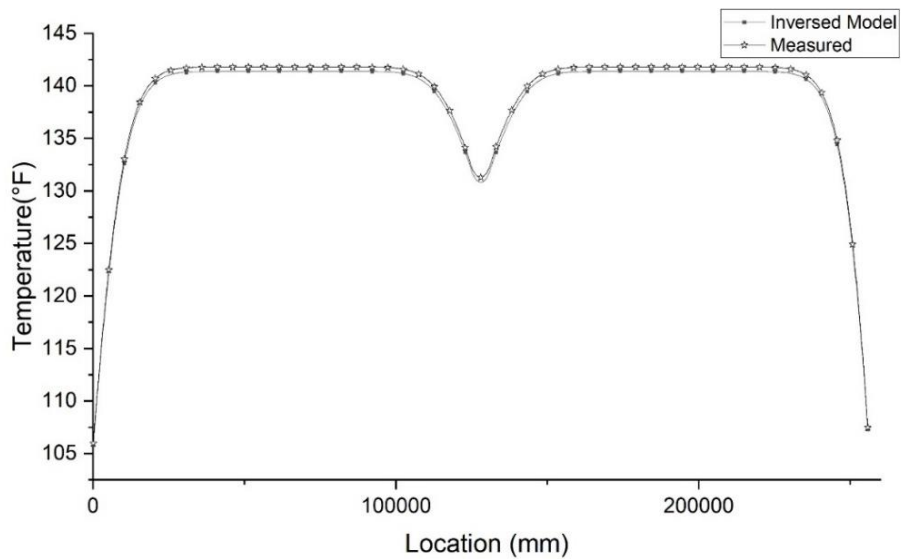


Figure 6. Comparison of measured temperature and inversed modeling

Fiber-optic sensor may not be able to measure the temperature at the center of the inclusion, we can draw a trend line by connecting the bottom of each concave to have a

similar plot as necking. An example of trend line is shown in Figure 8. The point that has the lowest temperature is the center of the inclusion.

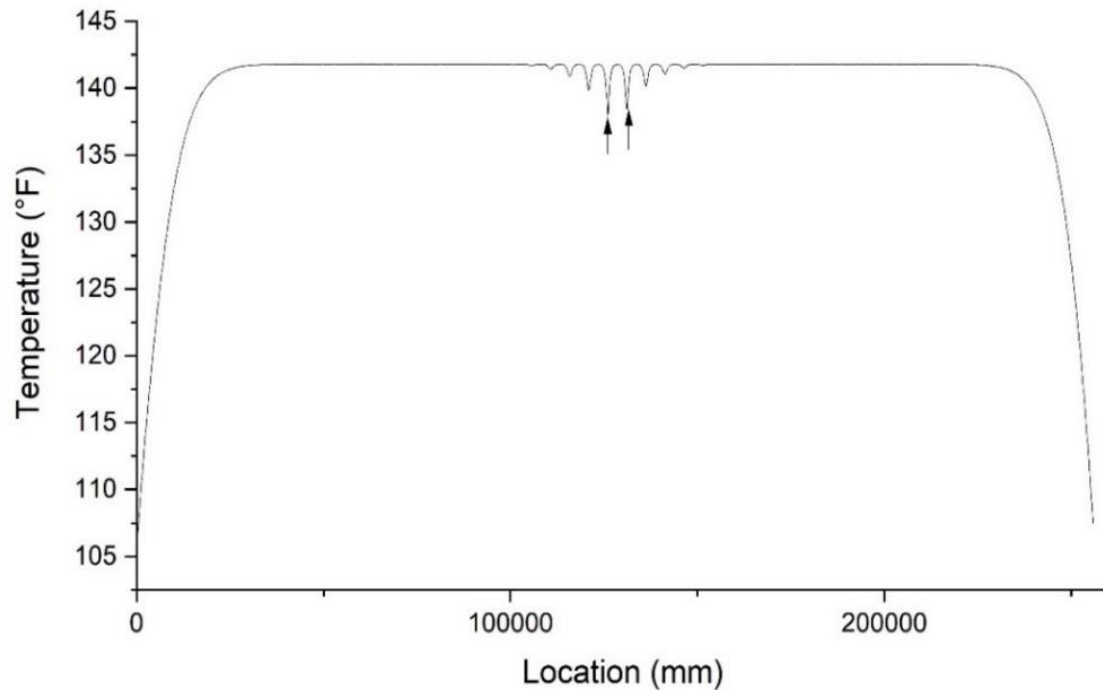


Figure 7. Temperature distribution of inclusion

Besides depth and height, we need the width at tangent direction to determine the size of an inclusion. The sketch of an inclusion is shown in Figure 9. The effective radius method is less accurate when estimating the size of an inclusion defect. The result usually underestimates the size at radial direction of the inclusion. Thus, a new method may be needed when estimating the size of inclusion. The height of the inclusion can be calculated with the similar method as the one for necking. Apply the method for the necking on this trend line to calculate the upper and lower boundary of the inclusion. Applying this method

to the one largest concave results in two points that represents the horizontal boundaries of the inclusion. The gap between the horizontal boundaries is the width of the inclusion. As for the depth, we assume it is equal to the width to simplify the calculation. After estimating the size of inclusion, we run a simulation and modify the depth accordingly to acquire a closer result. The comparison at the damaged region is shown in Figure 10.

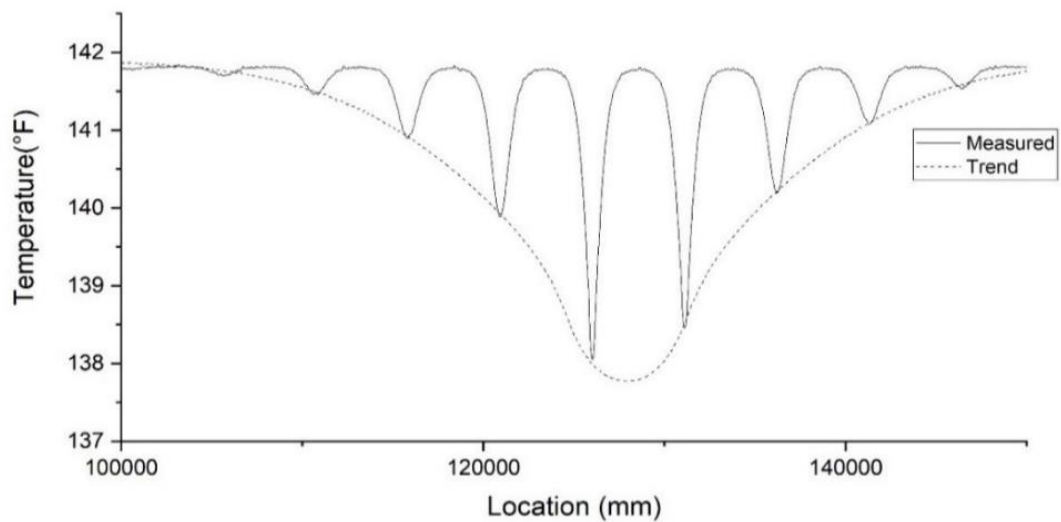


Figure 8. Trend line connecting each bottom point

To be noted that, this interpretation method may not accurately represent the actual geometry of the inclusion. On the horizontal plane, this method only determines the cross-section area rather than the actual geometry on the inclusion. We established two models with defects that have different length-width ratio but similar cross-section area. The temperature distribution is shown in Figure 11.

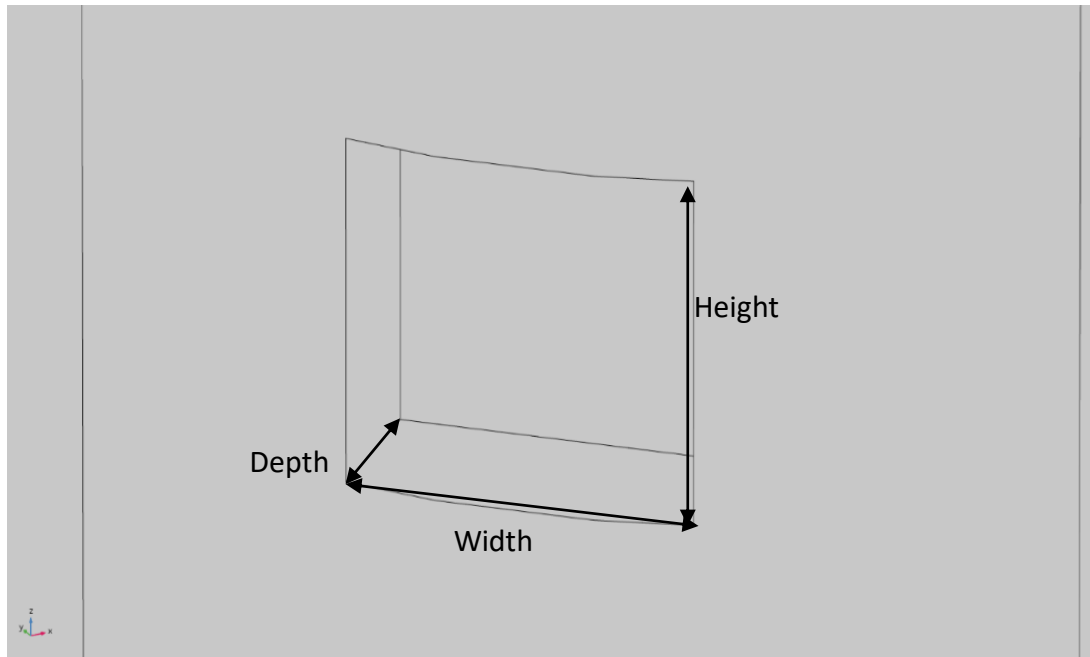


Figure 9. Sketch of inclusion

As shown in the figure, two models have similar temperature distribution within the shaft. This shows that defects that have same cross-section area could cause similar temperature anomaly. To determine the geometry of the inclusion, either tangent size or radial size has to be accurately estimated. However, the estimation is not accurate in most case. Tangent size determined using the above mentioned method is most accurate when fiber-optic sensor passes the exact center of the defect.

However, in most situations, optical fiber cannot have direction measurement of the temperature distribution at the center of the defect. In these situations, the tangent size determined by the plot is usually overestimated. The overestimated tangent size may further affect the estimation of radial size. In order to have a similar temperature distribution as the original data, adjustment on the radial direction results in underestimation on radial direction.

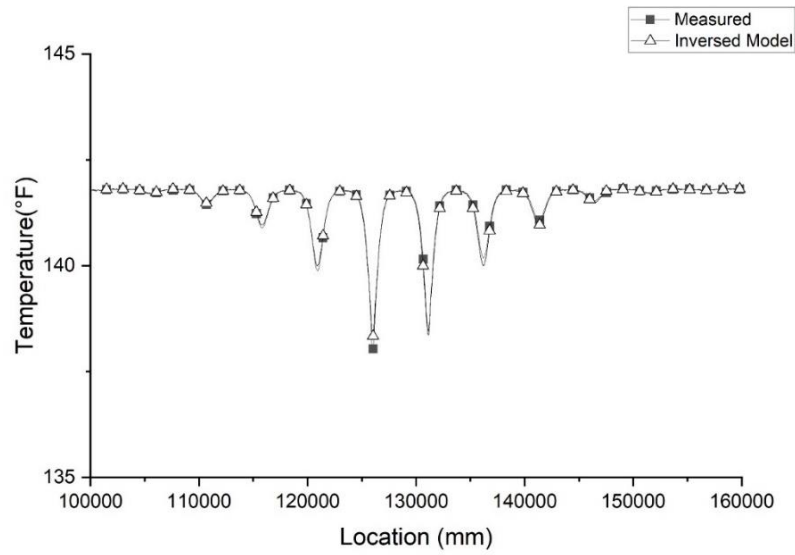


Figure 10. Comparison of measured temperature and inversed model of inclusion

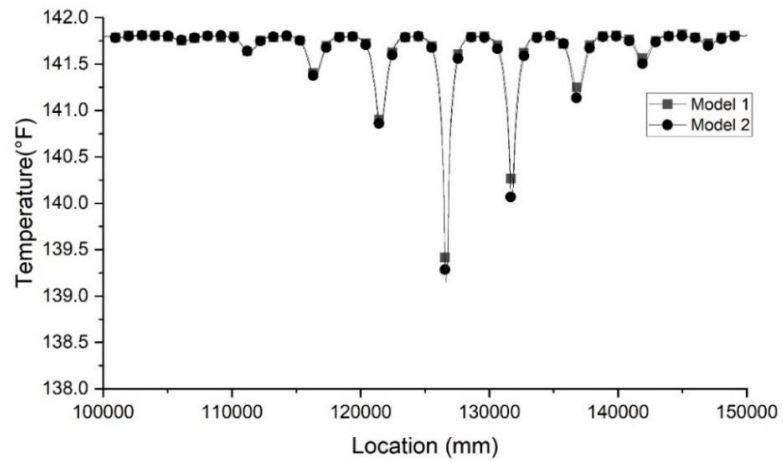


Figure 11. Comparison of two different cross-section shape but similar area

Overall, this method provides accurate prediction on area loss on the horizontal plane and size on vertical direction. Further study is needed to improve the way of interpretation.

4. CONCLUSIONS

The inverse modeling method proposed in this study cannot be achieved without the advance brought by the change of thermal couples to fiber-optic sensor. The more comprehensive temperature distribution data not only improve location prediction but also size prediction, especially for inclusion defect. For necking defect, the size prediction at radial direction made by effective radius method shows good agreement with the simulation result. The vertical size calculated using the method present in the result and discussion section is close to the vertical size of the defect. For the necking defect, the method presented has an accurate prediction of the defect.

For the inclusion defect, one more parameter is needed to determine the size of the defect, which is the size at the direction perpendicular to the radius on the horizontal plane. The temperature distribution plot of an inclusion has several continuous concaves depending on its vertical size. Connecting the bottom of each concave results in a trend line similar to the plot of a necking defect. Applying the method for necking on this trendline can determine the location and the vertical size of the defect. Using the method presented in result and discussion section can determine the size of cross-section. The temperature distribution of inverse model has good agreement with the temperature distribution data of the original model.

However, different inclusion that has similar cross-section area can conduct similar temperature distribution. In most case, overestimation on the tangent direction and underestimation on radial direction may happen. To have a more accurate inclusion prediction, the method to determine the geometry of the defect is still wanted.

REFERENCES

- [1.]Klingmuller O., and Kirsch, F., “Current practices and future trends in deep foundations,”*Reston, VA: American Society of Civil Engineers*, pp. 205, 2004.
- [2.]Dan Brown, Anton Schindler, “High performance concrete and drilled shaft construction,” *GSP 158 Contemporary Issues in Deep Foundations*, 2007.
- [3.]O’Neill M., “Integrity testing of foundations,” *Washington, D.C.: Transportation Research Board*, pp.6-13, 1991.
- [4.]Massoudi, N., and Teffera, W., “Non-destructive testing of piles using the low strain integrity method.” *Proc. 5th Int. Conf. on Case Histories in Geotechnical Engineering*, Missouri Univ. of Science and Technology, Rolla, MO, 13–17,2004.
- [5.]Ashlock, J.C., A.M. ASCE, Fotouhi, M.K., “Thermal integrity profiling and crosshole sonic logging of drilled shafts with artificial defects,” *Geo-Congress 2014 Technical Papers, GSP 234 © ASCE*, no. 1795, 2014.
- [6.]Sheng-Jen Hsieh, Robert Crane And Shamachary Sathish, “Understanding and predicting electronic vibration stress using ultrasound excitation, thermal profiling, and neural network modeling,” *Nondestructive Testing and Evaluation*, vol. 20, no. 2, pp.89-102, 2005.
- [7.]Johnson, K.R., MCE, E.I., “Temperature prediction modeling and thermal integrity profiling of drilled shaft,” *Geo-Congress*, 2017
- [8.]Zhong, R., Guo, R., Deng, W., “Optical-fiber-based smart concrete thermal integrity profiling: an example of concrete shaft,” *Advances in Materials Science and Engineering*, 2018
- [9.]Schindler, A., Folliard, K., “Heat of hydration models for cementitious materials,” *ACI Materials Journal*, vol. 102, no. 1, pp. 24-33, 2005.
- [10.]Liu, W., He, W., Zhang, Z., “A calculation method of thermal conductivity of soils,” *Journal of Glaciology and Geocryology*, vol. 24, no. 6, pp. 770-773, 2002.
- [11.]Cristina Sáez Blázquez, Arturo Farfán Martín, Ignacio Martín Nieto, etc. “Measuring of thermal conductivities of soils and rocks to be used in the calculation of a geothermal installation,” *Energies*, vol. 10, no. 795, pp. 1-19, 2017.
- [12.]Barry-Macaulay, D., Bouazza, A., Singh, R.M., “Thermal Conductivity of soils and rocks From the Melbourne (Australia) region,” *Engineering Geology*, no. 164, pp. 131-138. 2013.

III. INFLUENCE OF AGGREGATES IN CONCRETE ON OPTICAL-FIBER BASED THERMAL INTEGRITY PROFILING ANALYSIS

ABSTRACT

Fiber-optic sensor has drawn wide attention in the nondestructive testing of Civil Engineering materials due to its high accuracy and resolution as well as cost-efficiency. Currently, optical fiber as the sensor is proposed to conduct the thermal integrity profiling (TIP) of concrete. However, concrete is not a homogeneous material as assumed in current thermal modeling of TIP studies. Its essential components, such as aggregates may cause thermally heterogeneous problems when implementing fiber-optic sensor for TIP. Thus, an examination of potential influence and solutions to it is needed. In this paper, we use the concrete structure with different grades of aggregates to conduct numerical simulation for thermal modeling of nondestructive testing of concrete structures. The goal is to examine how the size of aggregates would influence the testing result. Firstly, we establish three concrete structure models with three different grades of aggregates based on the scenarios where these concrete structures will be used. Then we simulate the TIP test on these models and extract the temperature at the location where optical fiber would be installed. The effect caused by the inhomogeneity of aggregate size and distribution as well as the possible method to minimize the effect are evaluated in the paper. Overall, aggregates of concrete have a significant influence on the accuracy of TIP analysis, and defects could be veiled if no proper treatment to the data is implemented.

1. INTRODUCTION TO EFFECT OF AGGREGATES

Concrete is the most important Civil Engineering material in all over the world. From residential houses to highway bridges, numerous concrete structures are constructed and maintained every day. A key indicator of the structural safety is the integrity of the concrete. Thus, the integrity of the concrete structure should be monitored from its construction process throughout its service time. During the construction process, concrete could be easily foiled due to inappropriate procedures, especially for a cast-in-site concrete shaft. Concrete shafts, which bear and transfer the loading to the ground, play an important role in superstructure construction. However, slump, soft soil, misplacement of rebar cage, multiple factors would cause defects when pouring the concrete [1]. 15% of 5,000 to 10,000 tested concrete shafts have the indication of potential defects, and 5% of the tested shafts show indisputable defect signals [2,3]. Defects cannot be prevented during the construction completely since the excavation and concrete pouring are both blind processes. Thus, the integrity test to determine whether defects exist within the concrete shaft is critical for the evaluation of concrete structural safety. Even if the structure is intact after construction, concrete would still degrade over time, even dramatically during a fire hazard. Extreme high temperature causes the degradation of material properties and spalling which leads to degradation of mechanical property and integrity of concrete structures [29,30]. An appropriate method of monitoring concrete structures helps evaluation of remaining capacity.

Recent studies proposed multiple fiber-optic sensor applications in concrete structure integrity testing and monitoring due to its durability, accuracy, immunity to

electromagnetic interference, resistance to harsh environment and cost-efficiency. Despite the well-established application in strain measurement, researchers started to explore a new usage of optical fiber as a thermal sensor in an integrity test. Zhong et al. [10] was the first to suggest using the optical fiber in thermal integrity profiling (TIP) for drilled shafts to acquire higher resolution spatial data. TIP, which is a non-destructive method, makes use of cement hydration heat to examine the integrity of a concrete shaft. Any defect like inclusion, necking, will be shown as temperature anomaly in temperature measurement [11-12, 28]. Compared to the conventional method, the TIP can cover a larger area and provide a more comprehensive result. However, the accuracy of the TIP is limited by the number of sensors or access tubes within the concrete shaft. Thus, the paper proposed to use Rayleigh scattering within optical fiber to replace thermocouples or thermal probes to improve data quality [10]. The optical fibers can be wrapped spirally around the rebar cage due to its flexibility which reduces horizontal interval significantly and provides a more comprehensive temperature distribution within the concrete shaft. On the other hand, Bao et al. [31] proposed using pulse pre-pump Brillouin optical time domain analysis (PPP-BOTDA) as a temperature sensing method to measure spatially-distributed temperatures in reinforced concrete specimens exposed to fire. The remaining capacity of a concrete structure can be evaluated through thermo-mechanical analysis when the temperature distributions in-situ are known [32]. The current state of practice in fire analysis is to measure temperature using thermocouples, then estimate the temperature distributions within the structures. However, this method is costly, time-consuming, easily affected by electromagnetic interference, moisture, and unanticipated junctions [33]. Fiber-optic

sensor can overcome these deficiencies and provides more comprehensive temperature distribution data which is necessary for thermo-mechanical analysis.

However, most of the research did not take the influence of aggregates into account. Concrete is a multi-components composite material, that consists of aggregate and cement. Up to 60%-80% of the volume of concrete is aggregate. Generally, aggregates are classified into two groups: fine-grained aggregates and coarse aggregates. Due to economic reasons, lower usage of cement is preferred in order to lower the cost, which requires the aggregates to consist of a range of sizes rather than a uniform size. While this fulfills the economic and mechanical purpose, a range of sizes of aggregate introduces material-heterogeneity to concrete. Various sizes of aggregates cause variation in bulk composition which leads to macro heterogeneity in concrete [34]. Properties of concrete are related to the size, geometry, and distribution of aggregates [35]. The properties differences between cement and aggregates, like thermal conductivity and heat capacity, cause uneven temperature distribution after heated. Since the thermal integrity testing method relies on temperature anomalies to identify any defects that happen within the concrete structure, the variation of temperature caused by random aggregate distribution may lead to an overestimation or underestimation of a defect. However, the uniform aggregate was adopted when testing the feasibility of fiber-optic sensor applications in the integrity test. While the test results were promising, the specimens were less realistic. The Influence of aggregates should be tested thoroughly before introducing fiber-optic sensor into a real application.

The objective of this paper is to examine the influence of aggregates in concrete on TIP analysis. Three concrete structure models were established, two of which are for beams and one is for concrete shaft. Each model has different sizes of aggregates randomly

distributed within the structures. The sizes of aggregates are based on the scenarios these concrete structures will be employed. Then we simulate the TIP test on these models and extract the temperature at the location where optical fibers would be installed. Evaluation of the influence caused by the inhomogeneity of aggregate size and distribution and possible methods to minimize the effect are shown in the paper.

2. METHODOLOGY

In this section we will introduce methodology to examine the effect of aggregates.

2.1. GOVERNING EQUATION

The integrity testing method for either beams or concrete shafts predicts the existence of crack or the shape of foiled concrete structure based on the temperature distribution inside the material. The governing equation of temperature T distribution of the heat transfer module in solid is: (1)

$$\frac{\rho C_p \partial T}{\partial t} = \left[\frac{\partial}{\partial x} \left(k \frac{\partial T}{\partial x} \right) + \frac{\partial}{\partial y} \left(k \frac{\partial T}{\partial y} \right) + \frac{\partial}{\partial z} \left(k \frac{\partial T}{\partial z} \right) \right] + Q \quad (1)$$

where the heat generation rate of the material is represented by Q; the heat capacity of the material is represented by C_p ; the thermal conductivity of the material is represented by k.

2.2. HEAT TRANSFER IN AIR

In the beam models, concrete beams are not directly heated by an assigned heat source. To simulate a fire hazard simulation, the heat source is set a distance away from

the concrete beam. Thus, heat transfer is not limited to conduction which is the primary heat transfer way in a solid object. Conduction in air and radiation are two primary ways to transfer heat from the source to concrete beams. Convection in air and radiation can be determined by Equation (2)-(6):

$$\rho C_p u \cdot \nabla T + \nabla \cdot q = Q + Q_p + Q_{vd} \quad (2)$$

$$(1 - \varepsilon)G = J - \varepsilon e_b(T) \quad (3)$$

$$G = G_m(J) + G_{amb} + G_{ext} \quad (4)$$

$$G_{amb} = F_{amb} e_b(T_{amb}) \quad (5)$$

$$e_b(T) = n^2 \sigma T^4 \quad (6)$$

where n represents the refractive index, ε represents the emissivity of the surface.

2.3. HEAT GENERATION

In the drilled shaft model, the hydration heat generated during the concrete curing process is the key to the TIP test. Thus, it is necessary to determine the heat generation of concrete before simulation. The gross heat production and generation rate are two significant factors of temperature distribution.

Two factors together determine the temperature of the shaft and the performance of TIP. Both factors are related to the ingredient of cement. Changing the proportion of cement would generate a different amount of heat. The total heat production can be calculated by Equation (7) to (9) [23]:

$$Q_0 = Q_{cem}p_{cem} + 461p_{slag} + Q_{FA}p_{FA} \quad (7)$$

$$Q_{cem} = 500p_{C_3S} + 260p_{C_2S} + 866P_{C_3A} + 420p_{C_4AF} + 624p_{SO_3} + 1186p_{FreeCaO} + 850p_{MgO} \quad (8)$$

$$Q_{FA} = 1800p_{FACaO} \quad (9)$$

where p represents the weight fraction of each compound. The chemical composition of cement and fly ash are usually available from the supplier.

The rate of hydration can be calculated using the equation provided by Schindler and Folliard (2005):

$$\alpha(t) = \alpha_u \exp\left(-\left[\frac{\tau}{t_e}\right]^\beta\right) \quad (10)$$

$$\alpha_u = \frac{(1.031w/cm)}{(0.194+w/cm)} + 0.5p_{FA} + 0.3p_{SLAG} < 1 \quad (11)$$

$$\beta = p_{C_3S}^{0.227} \cdot 181.4 \cdot p_{C_3A}^{0.146} \cdot Blaine^{-0.535} \cdot p_{SO_3}^{0.558} \cdot \exp(-0.647p_{SLAG}) \quad (12)$$

$$\tau = p_{C_3S}^{-0.401} \cdot 66.78 \cdot p_{C_3A}^{-0.154} \cdot Blaine^{-0.804} \cdot p_{SO_3}^{-0.758} \cdot \exp(2.187 \cdot p_{SLAG} + 9.5 \cdot p_{FA} \cdot p_{FACaO}) \quad (13)$$

where $\alpha(t)$ represents the degree of hydration of cement at time t. And w/cm is a water-cement ratio. β and τ are determined by the cementitious constituent fractions. According to ASTM D7949-14, the recommended timing to perform TIP would be 12 hours after concrete placement until the number of days equivalent to foundation diameter in meters divided by 0.3 m.

2.4. HEAT TRANSFER IN SOIL

Heat is dissipated into surrounding soil after the heat is generated due to the hydration process. Since the predominant material in soil is solid, conduction plays the

most important role in heat dissipation in the shaft simulation. Aside from the temperature and density of the material, two factors control the conduction process, thermal conductivity, and heat capacity.

Soil is a composite material consisting of solids, air, and water. The effective thermal conductivity depends on the constitution of soil and the thermal conductivity of each phase. The thermal conductivity can be calculated by Equation (14) [24-26]:

$$k_1 = k_s - n[k_s - S_w k_w - (1 - S_w)k_a] \quad (14)$$

where n represents porosity, and S_w represents the degree of saturation.

The shape of void inside of soil has an effect on heat transfer as well. To take that effect into account, the shape factor $\chi = \sqrt{S_w}$ is introduced into the equation. Now the equation becomes:

$$k = \sqrt{S_w}\{k_s - n[k_s - S_w k_w - (1 - S_w)k_a]\} + (1 - \sqrt{S_w})k_a \quad (15)$$

The temperature of the soil is assumed to be the same among the three phases.

The heat required to raise the temperature of soil one degree can be calculated by the sum of three phases $C_s m_s + C_w m_w + C_g m_g$. The total mass of the soil is $m_s + m_w + m_g$.

Therefore, the effective heat capacity of soil can be calculated as follow:

$$C_p = \frac{C_s m_s + C_w m_w + C_g m_g}{m_s + m_w + m_g} \quad (16)$$

Considering that the mass of air is negligible, the equation can be simplified as:

$$C_p = \frac{C_s + C_w w}{1 + w} \quad (17)$$

2.5. AGGREGATE DISTRIBUTION

The aggregate distribution method used in the simulation is provided by Qian and Garboczi [36]. Concrete is considered a composite geometrical structure where aggregates like gravel are embedded in a mortar matrix. Although using non-spherical particles is more realistic, to simplify the calculation, inhomogeneity caused by the shape of aggregates is not considered. Spherical shape aggregate is adopted in this study. Each time an aggregate particle with a random radius is generated. The radius is determined by a pseudo-random number generator within a given range. Then the aggregate particles are placed at a random coordinate within a given range of coordinates which is the size of the model.

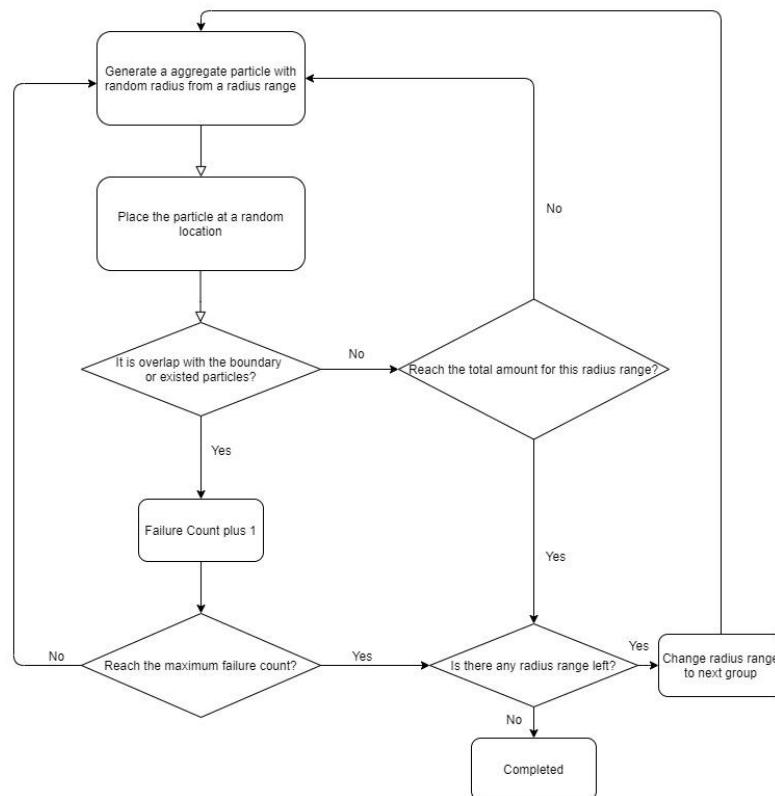


Figure 1. Flow chart of aggregate placement

The key algorithm required in the particle placing procedure is to check whether aggregate particles are overlapped. Since the shape of the particle is not considered, the overlap algorithm simply consists of equations to check if the distance between particles and the distance between particle and boundaries are smaller than zero. A variable is assigned to count the failure of placement. When the total amount of aggregate for a certain radius range is reached or the failure count exceeds the limit, the next radius range would be used for a new round of placement. The placement procedure will stop after all radius ranges are finished. The flow chart in Figure 1 demonstrates the procedure of aggregate placement.

2.6. SIMULATION PARAMETERS AND MODEL FOR BEAM

To simulate the temperature distribution within the beam exposed to a fire hazard environment, a 2-D model is established. The model is shown in Figure 2. The size of the model is 610mm×152mm. The model consists of three elements, gravel, sand, and cement. The circles with multiple colors represent aggregates, each color represents a radius range. The grey section represents cement surrounding aggregates. The small gap between aggregate represents the location of the fiber optic sensor. Rebar is not established in this model since the main focus is the effect of aggregate. Although is not shown in the figure, the beam model is surrounded by air with default properties in Comsol. The heat source is set at the bottom of the air section to simulate fire. The heat rate is set at several given rates. Temperature distribution data is acquired at the gap with a space interval of 1 cm. The properties of each component can be found in Table 1. Heat rate and duration can be found in Table 2.

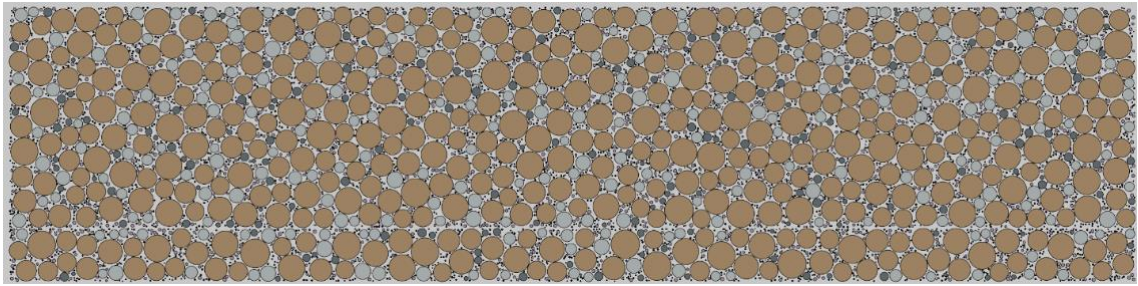


Figure 2. Geometry of beam model

2.7. SIMULATION PARAMETERS AND MODEL FOR SHAFT

To simulate the temperature evolution and distribution within the shaft, a 3D model is established as shown in Figure 3. Figure 3 shows the composition of a concrete shaft model. To be noted that the rebar cage is not established in the model. Rebar has relatively low heat capacity and high thermal conductivity, the heat that transfers into rebar cage is negligible. Moreover, the volume of the rebar cage is relatively small compared to the concrete shaft. To simplify the model, no rebar cage geometry is input to the model. However, it is still necessary to point out the location of the rebar cage.

In the paper proposed using fiber optic sensor as means to acquire temperature distribution data for TIP, the fiber optic sensor is wrapped around rebar cage. The location of the rebar cage in the model is where the temperature distribution data would be extracted. Optical fiber is not input to the geometry for a similar reason. The properties of concrete can be found in Table 1. The properties of soil can be found in Table 3. Figure 4 shows the steps for simulation. Following the steps shown in Figure 4 and input the parameters, the result in this paper should be reproduced.

Table 1. Properties of each component in beam model

	Volumetric Fraction	Density (kg/m^3)	Heat Capacity ($kJ/(kg \times K)$)	Thermal Conductivity ($W/(m \times K)$)
HCP	0.204	2160	1.55	1.163
Coarse Aggregate	0.7	2660	0.84	2.5
Fine Aggregate	0.082	2660	0.80	2
Air	0.014	1.225	1	0.0333

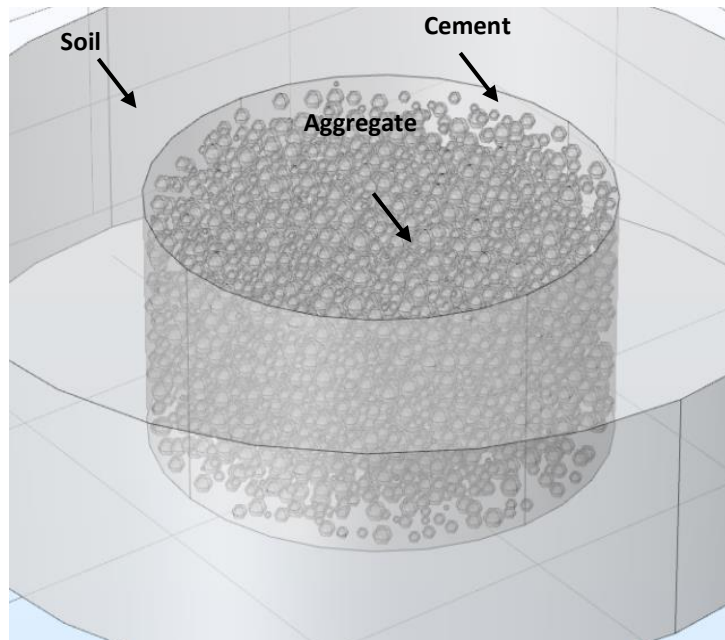


Figure 3. Shaft-soil model 3

Table 2. Heat rate and duration

Heat Rate	<i>25kW</i>	<i>40kW</i>	<i>80kW</i>
Duration	<i>45 min</i>	<i>10 min</i>	<i>10min</i>

Table 3. Soil properties 3

Properties	Unit	Value
Soil solid thermal conductivity	<i>W/m · K</i>	5.2
Water thermal conductivity	<i>W/m · K</i>	0.55
Air thermal conductivity	<i>W/m · K</i>	0.05
Density	<i>kg/m³</i>	1830
Soil solid heat capacity	<i>J/(kg · K)</i>	850
Water heat capacity	<i>J/(kg · K)</i>	4190
Water Content	%	39.8
Saturation	%	97
Porosity	%	51.1

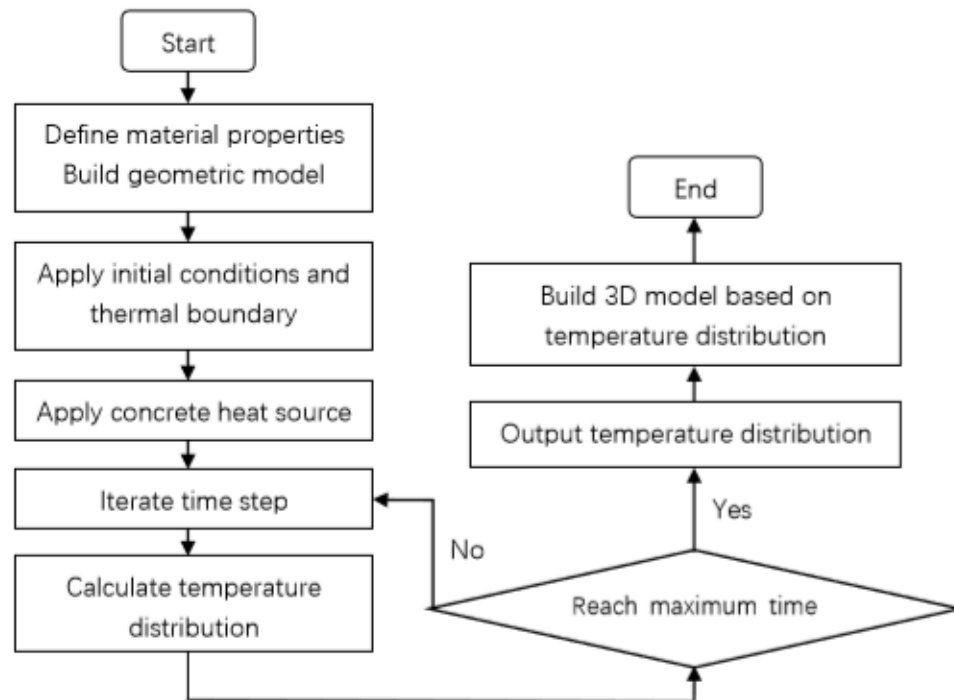


Figure 4. Simulation flow chart

3. RESULT AND DISCUSSION

The simulation result of two beam-models and one shaft model are presented in this section along with the discussion of effect from aggregate size.

3.1. RESULT OF SELF-CONSOLIDATING CONCRETE BEAM

SCC is a type of concrete of which predominant aggregate type is the fine aggregate. This type of concrete sacrifices economic efficiency for higher workability. Its high workability gives it the ability to flow into intricate spaces and congested reinforcement. Moreover, SCC does not require vibrators to compact concrete which improves safety and

reduces noise at the site. Since SCC has wide applications in the construction, SCC would be a standard material to study the effect of aggregate in concrete with small size aggregate.

The SCC in the simulation has a maximum grain size of 12 mm. The beam model is heated at the given heat rate in Paper II. After 65 min of heating and crack occurs, temperature data are extracted at the location of the virtual fiber-optic sensor.

Since our main focus is not the temperature distribution of the whole beam structure, only temperature distribution at a straight-line direction is extracted. Temperature distribution data along the fiber-optic sensor are shown in Figure 5. As shown in Figure 5, the temperature data has a main peak along with many minor fluctuations at other locations. The main peak, according to the paper published by Bao et al. [10], indicates the location of cracks which occurred due to extremely high temperatures.

The predominant heat transfer way in concrete is conduction before a crack appears. However, after crack appears, space in the crack is filled with hot air, which means the predominant heat transfer at that location would be convection and radiation. The heat transfer at that location has higher efficiency compared with the intact concrete cover. Therefore, the temperature rises dramatically around cracks and the fiber-optic sensor catches this temperature change.

The temperature fluctuation shown in Figure 5 indicates the inhomogeneity of concrete caused by the size and distribution of aggregates. Assuming that concrete is homogeneous, temperature distribution should be a straight line along the intact concrete cover.

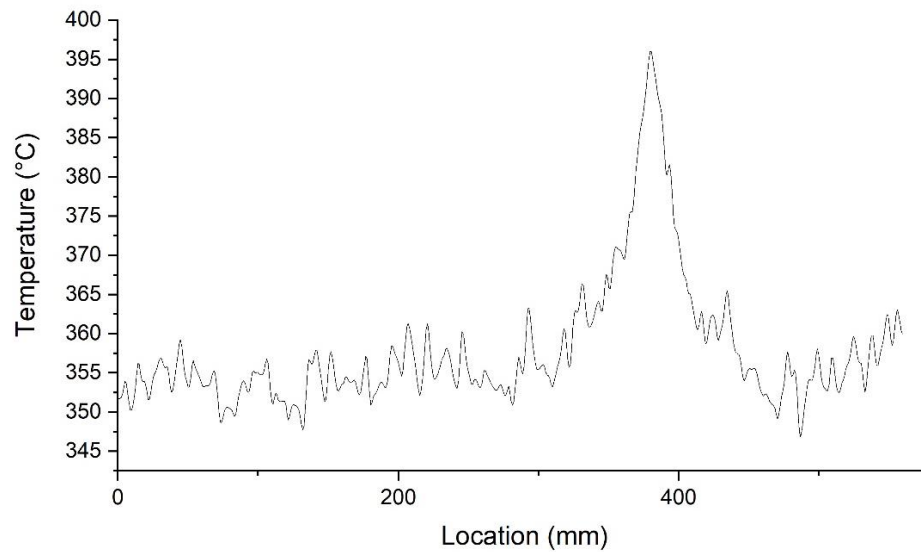


Figure 5. Temperature distribution of beam model 1

However, the thermal properties of cement are not the same as those of aggregates. Moreover, the spatial distribution is not even. These two factors make the heat conduction has a different rate in different directions, resulting in temperature fluctuation. The temperature increment is distinct compared to the fluctuation. This is because the size of the crack is considerably larger than the maximum grain size. The temperature increment due to cracking outgrows the effect caused by inhomogeneity. In the case of SCC, the effect of aggregate is insignificant.

3.2. RESULT OF CONVENTIONAL CONCRETE BEAM

Compared to the SCC beam, the CC beam is a more common case. The second case uses CC as the material of the beam. The maximum grain size in the CC is 26 mm. In this model, the CC beam is heated at the same condition as in the SCC model, and the temperature is also extracted at the same location at multiple different time. The

temperature data are shown in Figure 6a. The temperature fluctuation is considerably pronounced compared to the SCC model. The effect of aggregates increases with the increment of the maximum size of the aggregates. The fluctuation is almost twice as the one in the SCC model. The location of cracks is pointed in Figure 6a, and almost undetectable from the data. On the one hand, the size of the crack is slightly smaller compared to the SCC model, which decreases the increment caused by crack. On the other hand, the larger fluctuation due to larger aggregates makes it harder to recognize the crack. These two factors together result in a non-distinctive temperature increment shown in Figure 6a. The existence of coarse aggregates could be a problem for the application of the fiber-optic sensor in concrete structures. Although the location of defects cannot be detected based on the data at a certain time, there is still a solution to that problem. It should be noted that cracks are not naturally existed in the concrete structure. The crack in the model develops due to the exposure to extremely high temperatures. We can make use of the temporal temperature logging to solve this problem of non-distinctive data. Firstly, we divide temperature data into groups based on the time collected. Then we divide the temperature data at each group by the average temperature (T_{avg}) of that group. The outcome is shown in Figure 6b. We have a more direct comparison of temperature distribution at a different time compared to Figure 6a.

The temperature increment caused by crack can easily be detected with the help of reference data. The temperature distribution of a damaged concrete outside of the damaged region is lower than the intact concrete beam. This is because the temperature increment caused by crack rises the average temperature, which leads to a lower ratio at the intact region.

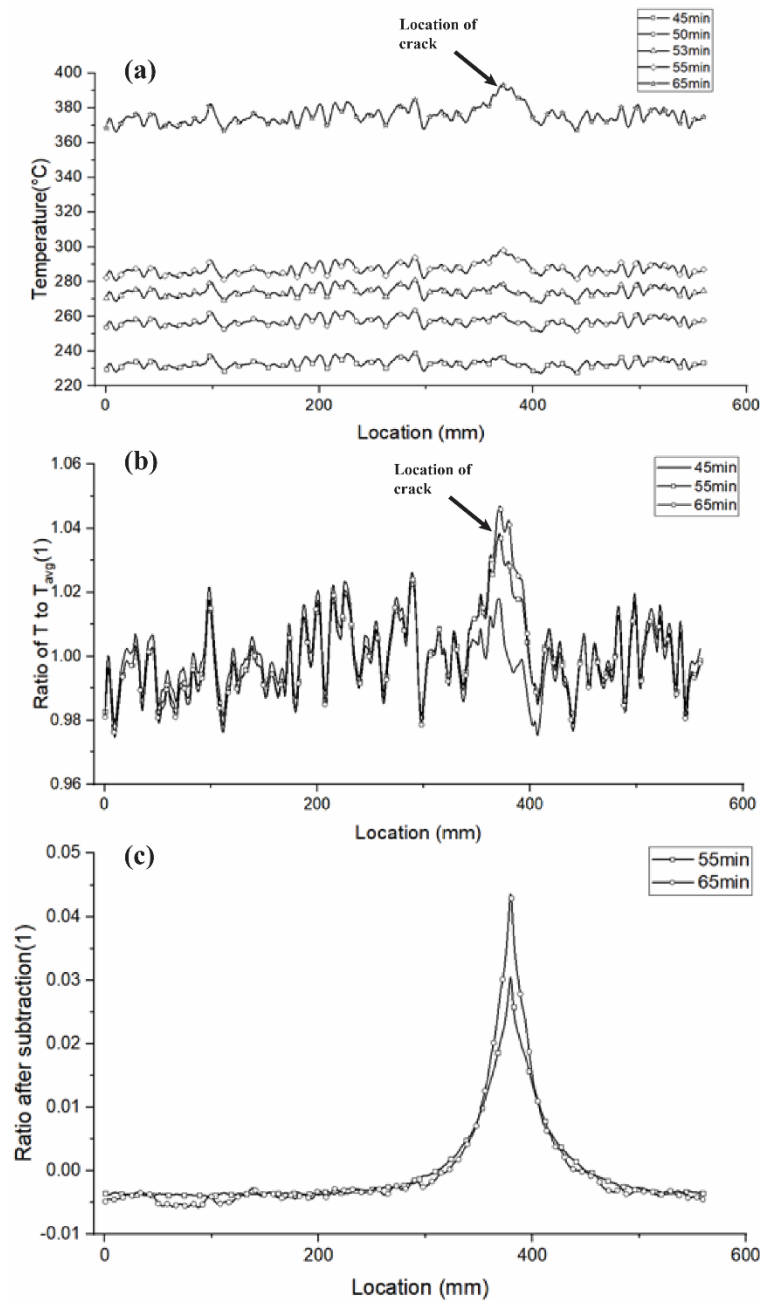


Figure 6. Temperature distribution.

(a) Temperature distribution of beam model 2, (b) normalized temperature distribution by T_{avg} , and (c) normalized temperature after subtraction

By subtracting the reference data from each group, we can further diminish the effect of aggregates. The result is shown in Figure 6c. The only peak in Figure 6c is the

temperature increment caused by crack. The intact region has an almost flat line which means the effect of aggregate is diminished.

3.3. SHAFT MODEL

The maximum grain size used in the current production shafts could be as large as 160 mm. Although 40 mm may be the most common case for concrete shaft, the maximum size of the shaft model is 80 mm to better study the effect of larger aggregate. To simulate the TIP test, we establish a 6-foot concrete shaft with a length of 1 m. Since the temperature anomaly is only restricted in the vicinity of the defect region, to simplify the calculation, only part of the concrete shaft nearby the defect is simulated in the model. The model geometry is shown in Figure 3. To simulate the inclusion defect in the concrete shaft, a 15inch×15inch×10inch sand block is placed at the circumference. The concrete shaft would generate heat during the curing process. Any location that has a shortage of concrete would generate less heat and be recognized as a thermal sink region at the plot. We simulate the 5-day curing process starting from pouring with 1-day interval. The temperature on the third day is recorded. The result is shown in Figure 7.

The fiber-optic sensor is wrapped around a rebar cage, the sensor may pass the abnormal region several times. Each concave region represents the temperature data fiber-optic sensor records in an abnormal region. As shown in the figure, two main concaves indicate the fiber-optic sensor passes the region for two times. The location that measures the lowest temperature represents the spot that is closest to the center of the anomaly. Even though it is not pronounced, temperature fluctuation can be found in the plot.

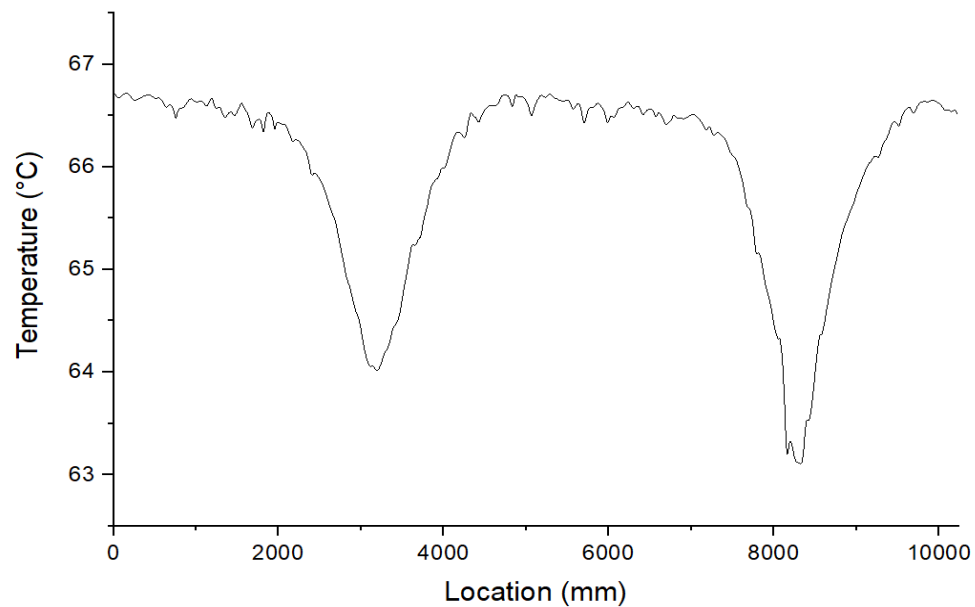


Figure 7. Temperature data of shaft model

The temperature anomalies outgrow the fluctuation even more than the case of SCC. The explanation would be that the defect size is much greater than the maximum size of aggregates. If we consider that each aggregate as a small inclusion, and the sand block as a single large inclusion, and temperature will change according to the size of inclusion. Then it is not hard to understand why the effect of aggregate is negligible. The ability to detect anomaly in the concrete shaft or other structure would be affected by aggregates only when the size of anomaly is similar or smaller to the maximum size of aggregates.

4. CONCLUSIONS

Based on the numerical simulation result and analysis, the following conclusions can be made:

The inhomogeneous due to the aggregates could cause temperature fluctuation. This fluctuation may conceal the temperature anomaly caused by the damaged region if the temperature-based testing method is employed. The larger the maximum aggregate size is, the larger the fluctuation would be. The ability to detect anomaly in the concrete shaft or other structure could be affected by aggregates when the size of anomaly is similar or smaller to the maximum size of aggregates. For the case of SCC or concrete shaft, the effect of aggregate is insignificant.

Even though temperature anomaly due to defects could be concealed by temperature fluctuation due to aggregates, with proper treatment, the effect of aggregates can still be diminished by using the temperature data of intact structure as a reference

The result indicates that the aggregates has the significant influence on superstructure when pouring with the conventional concrete. Proper treatment of the data can diminish the influence. All the results are based on numerical simulation, further verification by laboratory and in-situ testing is suggested in the future study.

REFERENCES

- [1.]O'Neill M., "Integrity testing of foundations," *Washington, D.C.: Transportation Research Board*, pp.6-13, 1991.
- [2.]Klingmuller O., and Kirsch, F., "Current practices and future trends in deep foundations," *Reston, VA: American Society of Civil Engineers*, pp. 205, 2004.
- [3.]Dan Brown, Anton Schindler, "High performance concrete and drilled shaft construction," *GSP 158 Contemporary Issues in Deep Foundations*, 2007.
- [4.]Kodur, V., Sultan, M. A., "Effect of temperature on thermal properties of high-strength concrete," *J.Mater. Civil Eng.*, 15(2), pp. 101-107, 2003.

- [5.]Kodur, V., Dwaikat, M., Raut, N., “Macroscopic FE model for tracing the fire response of reinforced concrete structures,” *Engineering Structures*, 31(10), pp. 2368-2379, 2009.
- [6.]Zhong, R., Guo, R., Deng, W., “Optical-fiber-based smart concrete thermal integrity profiling: an example of concrete shaft,” *Advances in Materials Science and Engineering*, 2018
- [7.]Mullins, G., “Thermal Integrity Profiling of Drilled Shafts,” *DFI Journal*, vol.4, no. 2, pp. 54-64, 2010.
- [8.]Mullins, G., “Advancements in drilled shaft construction, design, and quality assurance: the value of research,” *Technical Paper. International Journal of Pavement Research and Technology*, Vol.6, no.2, pp. 93-99, 2013
- [9.]Johnson, K. R., “Analyzing thermal integrity profiling data for drilled shaft evaluation,” *DFI Journal- The Journal of the Deep Foundations Institute*, Vol. 10, no.1, pp.25-33, 2016.
- [10.]Bao, Y., Hoehler, M. S., Smith, C. M., Bundy, M., Chen, G., “Temperature measurement and damage detection in concrete beams exposed to fire using PPP-BOTDA based fiber optic sensors,” *Smart Materials and Structures*, 2017.
- [11.]Usmani, A., Rotter, J. M., Lamont, S., Gillie, M., “Fundamental principles of structural behavior under thermal effects,” *Fire Safety Journal*, 36(8), pp. 721-744, 2001.
- [12.]Smalcerz, A., Przylucki, R., “Impact of electromagnetic field upon temperature measurement of induction heated charges,” *Int. J. Thermophys*, 34(4), pp. 667-679, 2013.
- [13.]Kreijger, P. C., “Inhomogeneity in concrete and its effect on degradation: a review of technology,” 1990.
- [14.]Shahbazi, S., Rasoolan, I., “Meso0scale finite element modeling of non-homogeneous three-phase concrete,” *Case Studies in Construction Materials*, vol.6, pp.29-42, 2017.
- [15.]Schindler, A., Folliard, K., “Heat of hydration models for cementitious materials,” *ACI Materials Journal*, vol. 102, no. 1, pp. 24-33, 2005.
- [16.]Liu, W., He, W., Zhang, Z., “A calculation method of thermal conductivity of soils,” *Journal of Glaciology and Geocryology*, vol. 24, no. 6, pp. 770-773, 2002.
- [17.]Cristina Sáez Blázquez, Arturo Farfán Martín, Ignacio Martín Nieto, etc. “Measuring of thermal conductivities of soils and rocks to be used in the calculation of a geothermal installation,” *Energies*, vol. 10, no. 795, pp. 1-19, 2017.

- [18.]Barry-Macaulay, D., Bouazza, A., Singh, R.M., “Thermal Conductivity of soils and rocks From the Melbourne (Australia) region,” *Engineering Geology*, no. 164, pp. 131-138. 2013.
- [19.]Qian, Z., Garboczi, E.J., “Anm: a geometrical model for the composite structure of mortar and concrete using real-shape particles,” *Materials and Structures*, vol. 39, pp. 149-158, 2016.

SECTION

2. CONCLUSION

In Paper I, we proposed an optical-fiber based TIP method. This method can be an improvement of infrared thermocouple probes and embedded sensor which are applied to conventional TIP by having high spatial resolution temperature data. The method also changes the way to deploy sensor from separated vertically deployed to spirally deployed around reinforcement cage. These two changes enable TIP to measure a high resolution and consistent temperature distribution within concrete shaft, leading to more accurate determination of integrity of concrete shaft.

The inverse modeling method proposed in Paper II cannot be achieved without the advance brought by the change of thermal couples to fiber-optic sensor. The more comprehensive temperature distribution data not only improve location prediction but also size prediction, especially for inclusion defect. For the necking defect, the method presented has an accurate prediction of the defect. For the inclusion defect, the temperature distribution plot of an inclusion has several continuous concaves depending on its vertical size. Connecting the bottom of each concave results in a trend line similar to the plot of a necking defect. Applying the method for necking on this trendline can determine the location and the vertical size of the defect. Using the method presented in result and discussion section can determine the size of cross-section. The temperature distribution of inverse model has good agreement with the temperature distribution data of the original model.

However, different inclusion that has similar cross-section area can conduct similar temperature distribution. In most case, overestimation on the tangent direction and underestimation on radial direction may happen. To have a more accurate inclusion prediction, the method to determine the geometry of the defect is still wanted.

In Paper III, we can draw conclusion as followed: The inhomogeneous due to the aggregates could cause temperature fluctuation. This fluctuation may conceal the temperature anomaly caused by the damaged region if the temperature-based testing method is employed. The larger the maximum aggregate size is, the larger the fluctuation would be. The ability to detect anomaly in the concrete shaft or other structure could be affected by aggregates when the size of anomaly is similar or smaller to the maximum size of aggregates. Proper treatment of the data can diminish the influence. All the results are based on numerical simulation, further verification by laboratory and in-situ testing is suggested in the future study.

VITA

Ruoyu Zhong graduated from South China University of Technology in Geotech in 2017. After graduation, he started his master's degree at Missouri University of Science and Technology under the supervision of Dr. Wen Deng. This research interest was the application of fiber-optic sensor on Civil Engineering materials, especially as thermal sensor. He earned his Master of Science in Civil Engineering from the Missouri University of Science and Technology in August of 2020.